

https://dspace.org/

Symmetry and numerical investigation of smectic liquid crystals

Dada, Kim

2009-05-21T08:28:00Z
http://hdl.handle.net/10539/6960

Downloaded from a DSpace repository. https://dspace.org/

Symmetry and Numerical Investigation of Smectic Liquid Crystals

MSc Dissertation

Kim Dada

0212542A

Supervisor: Prof. E Momoniat

Centre for Differential Equations, Continuum Mechanics and Applications

School of Computational and Applied Mathematics

University of the Witwatersrand

October 13, 2008

I declare that this dissertation is my own unaided work. It is being submitted for the degree of Masters of Science at the University of the Witwatersrand, Johannesburg. It has not been submitted before for any degree or examination at any other university.

Kim Bernadettte Dada

5 October 2008

Abstract

In this dissertation both smectic-A and smectic-C liquid crystals are discussed. A dynamic equation for modeling the behaviour of smectic-C liquid crystals under the effect of an electric field is derived. The analytical solution is obtained using Lie point symmetries. From this the steady-state solution is obtained. The model equation is solved using a finite difference approximation, the method of lines and pseudo-spectral methods. The solutions are compared for accuracy and efficiency.

Acknowledgments

I would like to thank my supervisor Prof. E. Momoniat for all his help and patience throughout my MSc. For always being available and showing great support. I would also like to thank Prof. D. Mason for useful discussions.

Dedication

I dedicate this MSc dissertation to my parents, to thank them for all the love and support they have given me.

TABLE OF CONTENTS

1. INTRODUCTION 13

1.1 PROPERTIES OF LIQUID CRYSTALS 13

1.2 APPLICATIONS OF LIQUID CRYSTALS 14

1.3 TYPES OF LIQUID CRYSTALS 16

1.3.1 NEMATIC LIQUID CRYSTALS 16

1.3.2 SMECTIC LIQUID CRYSTALS 17

2. DERIVATION OF THE NONDIMENSIONAL MODEL 23

2.1 DESCRIPTION OF THE PROBLEM 23

2.2 NONDIMENSIONAL DYNAMIC EQUATION 34

3. LIE POINT SYMMETRIES AND THE STEADY-STATE SOLUTION 36

3.1 LIE POINT SYMMETRIES 36

3.2 STEADY-STATE SOLUTION 41

4. PSEUDO-SPECTRAL METHODS 44

4.1 THE SINC METHOD 45

4.2 THE FOURIER METHOD 46

5. NUMERICAL SOLUTIONS 49

5.1 A FINITE DIFFERENCE APPROXIMATION 50

5.2 THE METHOD OF LINES 53

5.3 THE SINC METHOD 56

5.4 THE FOURIER METHOD 58

6. CONCLUSION AND FUTURE WORK 72

APPENDIX 76

BIBLIOGRAPHY 88

TABLE

6.1 **Running times of the different methods used in MATLAB** 73

LIST OF FIGURES

1.1 The long molecular axes of nematic liquid crystals tend to align parallel to each other along the director **n**. 16

1.2 The molecules are aligned parallel to the director along the z-axis, and perpendicular to the planes. 18

1.3 SmC liquid crystals arranged in well-defined layers. Molecules are tilted at an angle θ to the director **a**. 19

1.4 The director **n** makes an angle θ with the layer normal **a**. The unit vector **c** describes the direction of the molecules, which is parallel to the projection of **n** and perpendicular to **a**. 20

1.5 SmC* liquid crystals with spontaneous polarization **P**. The director **n** rotates around the fictitious cone. 21

2.1 The field is tilted at a constant angle $\alpha \geq 0$. 25

2.2 Right-handed orthonormal triad of vectors, **a**, **c** and **b**. 26

3.1 Approximate solutions of the nondimensional dynamic equation (2.52) using Lie point symmetries setting $d = 1$ and $s > 1$. The value for $f = \epsilon$ ranges from 0.0125 to 0.0625 and b_2 ranges from 0.1 to 0.5. These special cases arise from the general solution of (3.26) when $b_2 = 0$ and $v = d$. . 41

3.2 Numerical solution of (3.27) using *Mathematica* 43

3.3 Solution of the ordinary differential equation (3.27) which was solved numerically in *Mathematica*. 43

5.1 Numerical solution of the nondimensional dynamic model (2.52) shows erratic behaviour occurring at the boundaries. A non-smooth solution is obtained when using a finite difference approximation. 62

5.2 Numerical solution of the nondimensional dynamic model (2.52) using the method of lines with a small final time $t_{final} = 0.1$. The graph shows the rotation angle u is symmetric about the X-axis, and is decreasing with increasing magnitude of X. The boundary conditions at $u_0(T) = 0$ and $u_n(T)$ force the rotation angle to be zero. 63

5.3 Numerical solution of the nondimensional dynamic model (2.52) using the method of lines with a larger final time $t_{final} = 5$. The graph shows that the rotation angle u is symmetric about the X-axis and over a larger period of time it converges until a potential hill is reached. The boundary conditions at $u_0(T) = 0$ and $u_n(T)$ force u to be zero. 64

5.4 When polarization $\mathbf{P}$ is absent, the rotation angle u converges to a potential well over a period of time when using the method of lines. 65

5.5 Numerical solution of the nondimensional dynamic model (2.52) using the Sinc method with a small final time $t_{final} = 0.1$. The graph shows the rotation angle u is symmetric about the X-axis, and is decreasing with increasing magnitude of X. The boundary conditions at $u_1(T) = 0$ and $u_n(T)$ force the rotation angle to be zero. 66

5.6 Numerical solution of the nondimensional dynamic model (2.52) using the Sinc method with a larger final time $t_{final} = 5$. The graph shows that the rotation angle u is symmetric about the X-axis and over a larger period of time it converges until a potential hill is reached. The boundary conditions at $u_1(T) = 1$ and $u_n(T)$ force u to be zero. 67

5.7 When polarization $\mathbf{P}$ is absent from the problem, the rotation angle u (over time) converges to a potential well when using the Sinc method. . 68

5.8 Numerical solution of the nondimensional dynamic model (2.52) using the Fourier method with a small final time $t_{final} = 0.1$. The graph shows the rotation angle u is symmetric about the X-axis, and is decreasing with increasing magnitude of X. The boundary conditions at $u_1(T) = 0$ and $u_n(T)$ force the rotation angle to be zero. 69

5.9 Numerical solution of the nondimensional dynamic model (2.52) using the Fourier method with a larger final time $t_{final} = 5$. The graph shows that the rotation angle u is symmetric about the X-axis and over a larger period of time it converges until a potential hill is reached. The boundary conditions at $u_1(T) = 0$ and $u_n(T)$ force u to be zero. 70

5.10 When polarization $\mathbf{P}$ is absent, the rotation angle u (over time) converges to a potential well when using the Fourier method. 71

6.1 With $\alpha = 0; 2\pi; 4\pi...$, the electric field is parallel to the $X - y$ plane. . . 74

6.2 With $\alpha = \frac{\pi}{2}; \frac{3\pi}{2}; \frac{5\pi}{2}...$, the electric field is perpendicular to the $X - y$ plane. 75

6.3 With $\alpha = \pi; 3\pi; 5\pi...$, the electric field is parallel to the $X - y$ plane. . . 75

1. INTRODUCTION

In this section the composition of liquid crystals is discussed, as well as the different types that exist. A further discussion follows on how liquid crystals are applied in the real world.

1.1 PROPERTIES OF LIQUID CRYSTALS

Liquid crystals are considered to be condensed matter that exhibit both properties of crystalline solids and simple liquids [1]. The molecules arrange themselves in a crystal like manner, but flow like a liquid. As a consequence of this property, liquid crystals generally possess orientational order, while losing some or all of their positional order. Orientational order is defined to be a measure of the tendency of the molecules to align along a unit vector, known as the director, while positional order is the extent to which the position of an average molecule or group of molecules shows translational symmetry [2].

The amount of order in a liquid crystal is quite small relative to that of a crystal, but can be manipulated with mechanical, magnetic or electric forces. Liquid crystals are anisotropic fluids that consist of rod or disc-like organic molecules which tend to align themselves along a common axis in space known as the director **n** [3].

There are many different types of liquid crystal states, depending upon the amount of order in the material. The two main liquid crystal states are nematic and smectic liquid crystals. Smectic liquid crystals also consist of different types, namely, smectic-A,B,C,D,E,F,G,H and I [4]. The difference between these types of liquid crystals is the amount of order that they each possess.

1.2 APPLICATIONS OF LIQUID CRYSTALS

Since liquid crystals exhibit unique optical properties, i.e. they scatter light strongly, they are known to be useful in various applications, mainly in engineering and medicine. For over 20 years now, research into liquid crystals has contributed greatly to optical displays and screens.

The most common application is liquid crystal displays (LCD's). One of the main advantages of this application is due to the very small amounts of electric power needed. This technology has grown extensively from digital watches in the 80's and pocket calculators, to advanced flat screen computers and televisions [2]. This technology will soon replace cathode ray tube displays completely. LCD's are made up of nematic liquid crystals which are implemented in what is known as the twisted nematic effect [5]. The twisted nematic effect contains liquid crystals which are precisely aligned under the effect of an applied electric field. The molecules are twisted and untwisted allowing light through. Depending on the amount of voltage applied by the electric field, the liquid crystal cells can twist up to 90°, which will then block all light passing through. When no voltage is applied, full light is able to pass through [6].

The basic concept behind liquid crystal displays is a light source applied to a flat display device which is made up of a number of colour or monochrome pixels.

Another application is Liquid Crystal Thermometers [2], which are thermometers that contain heat sensitive liquid crystals in a plastic tube. The colour of liquid crystal changes according to different temperature changes, which makes it very useful for temperature measurement. This is far safer than mercury in a glass tube and has a much higher temperature range. Also, special devices using liquid crystals can be attached to the skin to show the different temperatures. This can detect problems such as tumors.

One of the most recent devices using liquid crystals is optical imaging [2]. Devices such as these are used in medical applications and in nondestructive mechanical testing of materials under stress. Light is applied to a photoconductor consisting of two layers, in between which there are liquid crystals. The light creates an electric field in the liquid crystal, and the image of the electric pattern can then be recorded. This is a new and important field of research that has applications in diverse fields, such as engineering, physics, chemistry, biology, medical research and pharmacy.

1.3 TYPES OF LIQUID CRYSTALS

1.3.1 NEMATIC LIQUID CRYSTALS

The nematic phase is the simplest state of liquid crystals. The word nematic originates from the Greek word meaning thread. This is because when nematic liquid crystals are viewed under a polarized microscope, a thread like texture is observed. Nematics are polarizable rod-like organic molecules on the order of around 20 Å in length [7]. This phase has a similar structure to isotropic liquids, with the exception of the molecules aligning in a parallel manner along a common director **n**, which can be described by a unit vector parallel to the z-axis (see Fig. 1.1). Positional order is lost while

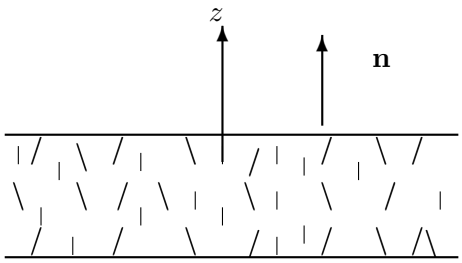

Fig. 1.1: The long molecular axes of nematic liquid crystals tend to align parallel to each other along the director **n**.

orientational order is maintained. In practice, the orientation of individual molecules differ to a large extent from the common direction, so the director must be better defined as the symmetry axis of the orientational distribution. Nematics are uniaxial, i.e. the distribution function is rotationally symmetric around the director [7].

1.3.2 SMECTIC LIQUID CRYSTALS

The word smectic comes from the Greek word meaning soap. This is because the thick slippery residual at the bottom of a soap dish is a type of smectic liquid crystal. Smectic phases have more degrees of order in comparison to those of nematic phases and they are found at lower temperatures. Smectic liquid crystals possess translational order, which is a condition where the molecules have some arrangement in space. (Crystals possess three degrees of translational order while liquids have no translational order.) Translational order is absent in nematics. Hence this increased order in smectic liquid crystals shows they are more solid-like than nematics [2].

Molecules in this smectic phase are arranged in well-defined, equally spaced layers. They move only within these layers while the layers themselves slide over one another like soap. Within the layers the molecules tend to align in the same direction described by the director $\mathbf{n}$. This director $\mathbf{n}$ makes an angle θ with the layer normal $\mathbf{a}$. θ is referred to as the smectic tilt angle and is usually temperature dependent. However it may vary due to competition between boundary conditions, elastic effects or smectic layer compressional effects [8]. It was shown in [9] that θ increases as temperature decreases.

As mentioned previously, there are different types of smectic phases. Two main types which will be discussed are smectic-A (SmA) and smectic-C (SmC) liquid crystals. To date very little research has been done on smectic-B, D, E, F, G, H and I liquid crystals.

SMECTIC-A LIQUID CRYSTALS

In this phase the director **n** is perpendicular to the smectic plane and parallel to the layer normal **a** of the molecules. In the idealized SmA phase the smectic tilt angle θ is equal to zero (see Fig. 1.2).
Each equally spaced layer is a two dimensional liquid. Within the layers the centre of gravity of the molecules possesses no long range order.

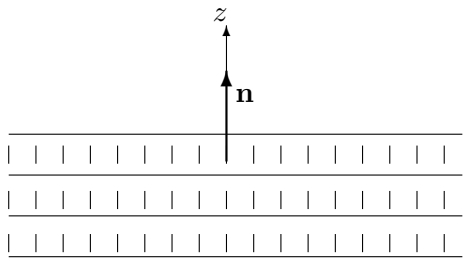

Fig. 1.2: The molecules are aligned parallel to the director along the z-axis, and perpendicular to the planes.

SMECTIC-C LIQUID CRYSTALS

Smectic-C liquid crystals also consist of elongated rod-like molecules which can be easily polarized due to their dipole substituents. This phase is formed when the directors of the liquid crystals tilt away from the layer normal at an angle θ as shown in Fig. 1.3. From X-ray diffraction it is shown that molecules are randomly arranged within structured layers. The molecules only move within the layers while the layers slide over one another. It is assumed that the tilt directions of the molecules align in the same direction.

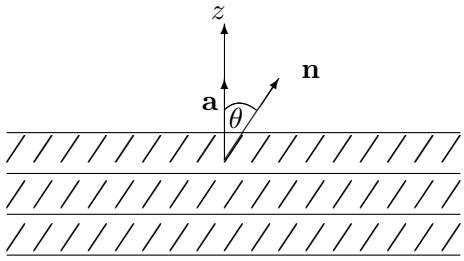

Fig. 1.3: SmC liquid crystals arranged in well-defined layers. Molecules are tilted at an angle θ to the director **a**.

X-ray experiments show the thickness of the layers to be $d = l\cos\theta$, where l is the length of the molecule, normally between 20 and 80 Å [3], and θ is the tilt angle. Since the molecules in this phase rotate rapidly about their long molecular axes and because of possible polarization field effects, SmC is said to be biaxial (i.e. 2D unstructured layers with a tilted molecular arrangement). Within the layers, molecules are said to rotate about the z-axis in a cone-shape as illustrated in Fig. 1.4.

A unit vector **n** (see Fig. 1.1) represents the projection of the molecules. Although at a given temperature the tilt angle θ is constant, the direction is not specified and is chosen at will. This direction may be described by an orthogonal unit projection **c** onto the plane of the layers, and is known as the c-director of the structure. It is perpendicular to layer normal **a** and parallel to the director **n** [10], as indicated in Fig. 1.4. ϕ is known as the orientation angle of **c** from the x-axis. This angle describes the orientation of the director **n**. i.e. the position of the liquid crystal rotating around the

z-axis projected onto the $x - y$ plane.

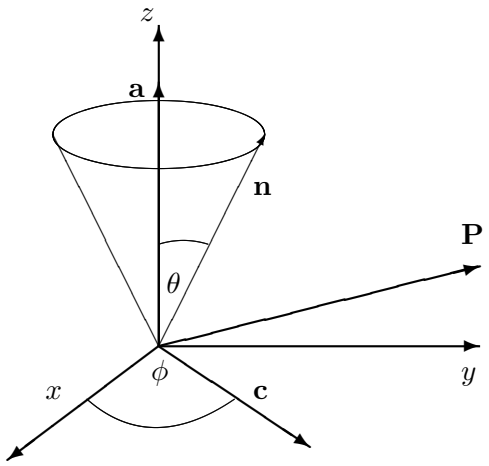

Fig. 1.4: The director **n** makes an angle θ with the layer normal **a**. The unit vector **c** describes the direction of the molecules, which is parallel to the projection of **n** and perpendicular to **a**.

When the molecules in this phase are chiral, i.e. they differ from their mirror image, they are next to each other in a skewed orientation. Chiral refers to the unique ability to selectively reflect one component of circularly polarized light [2, 3]. This state is referred to as the smectic-C* (SmC*) phase. Experiments have shown that SmC* liquid crystals are ferroelectric, which means they are substances which obtain spontaneous electric polarization, **P** [3]. The polarization exists parallel to the smectic layers and perpendicular to the molecules, and the magnitude is determined by molecular considerations although its existence depends only on symmetry [9]. Just as in the SmC phase, the director in the SmC* phase makes an angle θ with respect to the layer normal. The difference is that θ rotates from layer to layer producing a helical structure (see Fig. 1.5). The director in this phase is neither parallel nor perpendicular to the layers, but rotates from one layer to the next and

always lies on the surface of the fictitious cone.

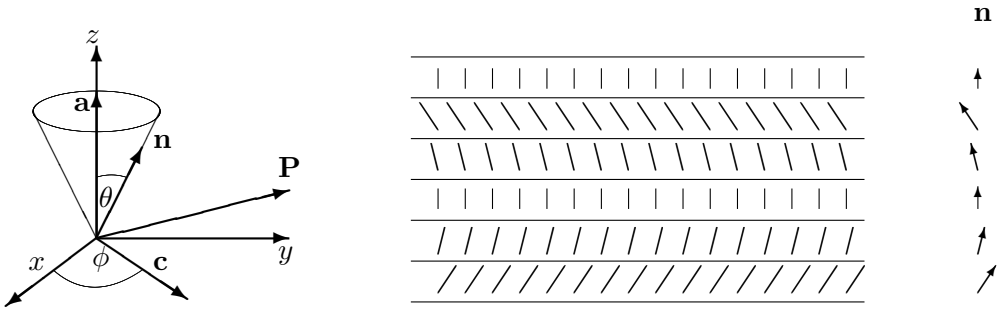

Fig. 1.5: SmC* liquid crystals with spontaneous polarization **P**. The director **n** rotates around the fictitious cone.

The study of liquid crystals is a very recent field of research and is continuing to grow at a rapid rate. Recent papers that deal with this subject are [11, 12].

In this dissertation we consider a nonlinear diffusion equation that models the effect of an applied electric field across a sample of smectic-C (SmC) liquid crystals. One of the main reasons SmC liquid crystals are considered here is due to their strong ferroelectricity, that is, they exhibit a spontaneous electric polarization in which the direction between the states can be switched by applying an external electric field [13]. The nonlinear partial differential equation that is obtained is solved numerically using a finite difference approximation, the method of lines and pseudo-spectral methods which include Sinc and Fourier methods. We compare the accuracy and efficiency of four algorithms. From the results obtained the finite difference schemes have poor convergence at the boundaries whereas the other three techniques converge. They converge to the steady-state solutions obtained [10].

This dissertation is divided up as follows. In section 2 the nonlinear model is derived and nondimensionalized. In section 3 the nondimensional equation is solved using Lie point symmetries to obtain the analytical solution of the model and the steady-state solution is obtained which is compared to the numerical solution. section 4 discusses the pseudo-spectral methods used to solve the nondimensional equation. In section 5 the model is solved by using numerical techniques. In section 6 concluding remarks are made and possible future research is mentioned.

2. DERIVATION OF THE NONDIMENSIONAL MODEL

In this section a detailed, step by step derivation of a model which describes a sample of SmC liquid crystals under the application of an externally applied electric field. This model is then nondimensionalized.

2.1 DESCRIPTION OF THE PROBLEM

In this problem an external electric field is applied to a sample of SmC* liquid crystals. Temperature remains constant so that θ is constant. The dynamic theory for SmC* liquid crystals is based on the conservation laws for mass and linear and angular momentum. From Fig. 1.4 it can be seen that

$$\mathbf{n} = \mathbf{a}\cos\theta + \mathbf{c}\sin\theta, \tag{2.1}$$

where $\mathbf{a}$ is fixed.

From Fig. 1.4, the following can be set

$$\mathbf{a} = (0, 0, 1), \tag{2.2}$$

$$\mathbf{c} = (\cos\phi(x,t), \sin\phi(x,t), 0). \tag{2.3}$$

It is now useful to introduce a third unit vector $\mathbf{b}$, where $\mathbf{b}$ is defined as $\mathbf{b} = \mathbf{a}\times\mathbf{c}$. Hence

$$\mathbf{b} = (-\sin\phi(x,t), \cos\phi(x,t), 0). \tag{2.4}$$

The orientation angle ϕ is only dependent on x and t.

The directors **a** and **c** are subject to the four constraints of SmC continuum theory [14]:

$$\mathbf{a}\cdot\mathbf{a} = 1,\ \mathbf{c}\cdot\mathbf{c} = 1,\ \mathbf{a}\cdot\mathbf{c} = 0 \text{ and } \nabla\times\mathbf{a} = \mathbf{0}.$$

Each of these constraints can easily be proved (see Appendix).
The spontaneous polarization, which is a characteristic of SmC liquid crystals, is in the same direction as **b** and is denoted by

$$\mathbf{P} = P_0\mathbf{b}, \tag{2.5}$$

where $P_0 > 0$ is the magnitude of the polarization. **P** may be positive or negative, according to the sign of **b**.

An external electric field **E**, is applied across a sample of SmC liquid crystals (see Fig. 2.1) and is given by

$$\mathbf{E} = E_0\left(1 + \frac{\epsilon}{2}\cos(\omega\epsilon t)\right)(\cos\alpha, 0, \sin\alpha), \tag{2.6}$$

where $0 < \alpha \ll 1$, and E_0 is the magnitude of the electric field.
E varies according to time and has an oscillating amplitude of $\frac{\epsilon}{2}$. In this derivation ϵ will be set equal to zero.

Total electric energy density that occurs when the electric field is applied across a liquid crystal is [1, 10]:

$$\omega_{elec} = -\mathbf{P}\cdot\mathbf{E} - \frac{1}{2}\epsilon_0\epsilon_a(\mathbf{n}\cdot\mathbf{E})^2, \tag{2.7}$$

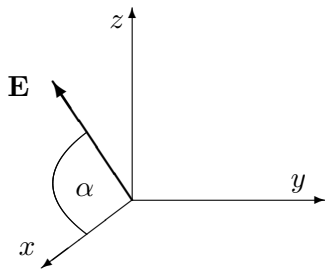

Fig. 2.1: The field is tilted at a constant angle $\alpha \geq 0$.

where $\epsilon_0 = 8.854\times10^{-12} F.m^{-1}$ is the permittivity of free space and ϵ_a is the dielectric anisotropy [15].

From the SmC constraints [14] and the equation for the applied electric field, ω_{elec}, we have

$$\begin{aligned}
\omega_{elec} &= -P_0(-\sin\phi, \cos\phi, 0)\cdot E_0(\cos\alpha, 0, \sin\alpha) \\
&\quad -\frac{1}{2}\epsilon_0\epsilon_a((0,0,1)\cos\theta + (\cos\phi, \sin\phi, 0)\sin\theta)\cdot(E_0(\cos\alpha, 0, \sin\alpha))^2 \\
&= P_0 \sin\phi E_0 \cos\alpha + (-P_0\cos\phi(0)) + 0 - \frac{1}{2}\epsilon_0\epsilon_a((0,0,\cos\theta) \\
&\quad +(\cos\phi\sin\theta, \sin\phi\sin\theta, 0)\cdot(E_0\cos\alpha, 0, E_0\sin\alpha))^2 \\
&= P_0 E_0 \sin\phi\cos\alpha \\
&\quad -\frac{1}{2}\epsilon_0\epsilon_a((\cos\phi\sin\theta, \sin\phi\sin\theta, \cos\theta)\cdot(E_0\cos\alpha, 0, 0, E_0\sin\alpha))^2 \\
&= P_0 E_0 \sin\phi\cos\alpha - \frac{1}{2}\epsilon_0\epsilon_a(E_0\cos\phi\sin\theta\cos\alpha + E_0\cos\theta\sin\alpha))^2 \\
&= P_0 E_0 \sin\phi\cos\alpha - \frac{1}{2}\epsilon_0\epsilon_a E_0^2(\cos\phi\sin\theta\cos\alpha + \cos\theta\sin\alpha)^2. \qquad (2.8)
\end{aligned}$$

The bulk energy density is

$$\omega_{bulk} = \frac{1}{2} B_3 \left(\frac{\partial \phi}{\partial x} \right)^2 , \tag{2.9}$$

where B_3 is the positive elastic constant related to the rotation of the c-director observed from layer to layer. The derivation is as follows:

$$\begin{aligned} 2\omega \;=\; & K_1(\nabla \cdot \mathbf{a})^2 + K_2(\nabla \cdot \mathbf{c})^2 + K_3(\mathbf{a} \cdot \nabla \times \mathbf{c})^2 + K_4(\mathbf{c} \cdot \nabla \times \mathbf{c})^2 \\ & + K_5(\mathbf{b} \cdot \nabla \times \mathbf{c})^2 + 2K_6(\nabla \cdot \mathbf{a})(\mathbf{b} \cdot \nabla \times \mathbf{c}) + 2K_7(\mathbf{a} \cdot \nabla \times \mathbf{c})(\mathbf{c} \cdot \nabla \times \mathbf{c}) \\ & + 2K_8(\nabla \cdot \mathbf{c})(\mathbf{b} \cdot \nabla \times \mathbf{c}) + 2K_9(\nabla \cdot \mathbf{a})(\nabla \cdot \mathbf{c}). \end{aligned} \tag{2.10}$$

where the K_i's are elastic constants [16]. We wish to write (2.10) in cartesian components.

Consider a right-handed orthonormal triad of vectors **a**, **c** and **b**, (see Fig. 2.2), so that

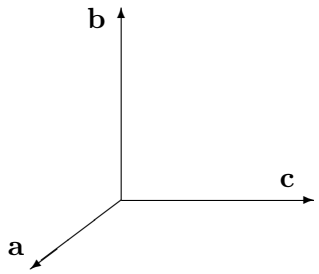

Fig. 2.2: Right-handed orthonormal triad of vectors, **a**, **c** and **b**.

$$\mathbf{a} = \mathbf{c} \times \mathbf{b}, \quad \mathbf{b} = \mathbf{a} \times \mathbf{c}, \quad \mathbf{c} = \mathbf{b} \times \mathbf{a}. \tag{2.11}$$

These relationships and the constraints on **a** will allow us to show that

- $\mathbf{a} \cdot \nabla \times \mathbf{c} = -b_{j,j}.$ (2.12)
- $\mathbf{b} \cdot \nabla \times \mathbf{c} = c_i a_{i,j} c_j.$ (2.13)
- $\mathbf{c} \cdot \nabla \times \mathbf{c} = a_i c_{i,j} b_j - b_i c_{i,j} a_j.$ (2.14)
- $\mathbf{a} \cdot \nabla \times \mathbf{b} = c_{i,i}.$ (2.15)
- $\mathbf{b} \cdot \nabla \times \mathbf{b} = c_i b_{i,j} a_j - a_i b_{i,j} c_j.$ (2.16)
- $\mathbf{c} \cdot \nabla \times \mathbf{b} = c_i a_{i,j} c_j - a_{i,i}.$ (2.17)

Proof of each of these relationships is given in the appendix.

Furthermore from [16] we have,

$$\begin{aligned}
\mathbf{b} \cdot \nabla \times \mathbf{c} &= c_i a_{i,j} c_j, && (2.18)\\
(\mathbf{a} \cdot \nabla \times \mathbf{c})^2 &= c_{i,j} c_j c_{i,k} c_k - (c_i a_{i,j} c_j)^2, && (2.19)\\
(\mathbf{c} \cdot \nabla \times \mathbf{c})^2 &= c_{i,j} c_{i,j} - c_{i,j} c_j c_{i,k} c_k - (c_{i,i})^2 + S_1, && (2.20)\\
(\mathbf{a} \cdot \nabla \times \mathbf{c})(\mathbf{c} \cdot \nabla \times \mathbf{c}) &= -c_{i,j} c_j c_{i,k} a_k - c_{i,i}(c_j a_{j,k} c_k) + S_2. && (2.21)
\end{aligned}$$

By substituting the above expressions into (2.10) we obtain

$$\begin{aligned}
2\omega &= K_1 (a_{i,i})^2 + (K_2 - K_4)(c_{i,i})^2 + (K_3 - K_4) c_{i,j} c_j c_{i,k} c_k + K_4 c_{i,j} c_{i,j} \\
&\quad + (K_5 - K_3)(c_i a_{i,j} c_j)^2 + 2K_6 a_{i,i}(c_j a_{j,k} c_k) - 2K_7 c_{i,j} c_j c_{i,k} a_k \\
&\quad + 2(K_8 - K_7) c_{i,i}(c_j a_{j,k} c_k) + 2K_9 a_{i,i} c_{j,j}. \qquad (2.22)
\end{aligned}$$

It has been shown in [16] that the elastic constants K_i are related to the

Orsay constants. Through the following relationships

$$\begin{aligned} K_1 &= A_{21}, \\ K_2 &= B_2, \\ K_3 &= B_1, \\ K_4 &= B_3, \\ K_5 &= 2A_{11} + A_{12} + A_{21} + B_3, \\ 2K_6 &= -(2A_{11} + 2A_{21} + B_3), \\ K_7 &= -B_{13}, \\ K_8 &= C_1 + C_2 - B_{13}, \\ K_9 &= -C_2, \end{aligned} \tag{2.23}$$

and by considering (2.22), the following equation for ω is obtained,

$$\begin{aligned} \omega &= \frac{1}{2}A_{21}(a_{i,i})^2 + \frac{1}{2}(B_2 - B_3)(c_{i,i})^2 + \frac{1}{2}(B_1 - B_3)c_{i,j}c_jc_{i,k}c_k \\ &+\frac{1}{2}B_3c_{i,j}c_{i,j} + \frac{1}{2}(A_{12} + A_{21} + 2A_{11} - B_1 + B_3)(c_ia_{i,j}c_j)^2 \\ &-\frac{1}{2}(2A_{11} + 2A_{21} + B_3)a_{i,i}(c_ja_{j,k}c_k) \\ &+B_{13}c_{i,j}c_jc_{i,k}a_k + (C_1 + C_2)c_{i,i}(c_ja_{j,k}c_k) + C_2a_{i,i}c_{j,j}. \end{aligned} \tag{2.24}$$

Here A_i, B_i and C_i are elastic constants.

From (2.7)

$$\begin{aligned} \omega_{elec} &= -\mathbf{P}\cdot\mathbf{E} - \frac{1}{2}\epsilon_0\epsilon_a(\mathbf{n}\cdot\mathbf{E})^2 \\ &= -\mathbf{P}\cdot\mathbf{E} - \frac{1}{2}\epsilon_0\epsilon_a((\mathbf{a}\cos\theta + \mathbf{c}\sin\theta)\cdot\mathbf{E})^2. \end{aligned} \tag{2.25}$$

Now set

$$\begin{aligned}
\mathbf{W} &= \omega + \omega_{elec} \qquad (2.26)\\
\Rightarrow \mathbf{W} &= \frac{1}{2}A_{21}(a_{i,i})^2 + \frac{1}{2}(B_2 - B_3)(c_{i,i})^2 + \frac{1}{2}(B_1 - B_3)c_{i,j}c_jc_{i,k}c_k\\
&\quad + \frac{1}{2}B_3c_{i,j}c_{i,j} + \frac{1}{2}(A_{12} + A_{21} + 2A_{11} - B_1 + B_3)(c_ia_{i,j}c_j)^2\\
&\quad - \frac{1}{2}(2A_{11} + 2A_{21} + B_3)a_{i,i}(c_ja_{j,k}c_k)\\
&\quad + B_{13}c_{i,j}c_jc_{i,k}a_k + (C_1 + C_2)c_{i,i}(c_ja_{j,k}c_k) + C_2a_{i,i}c_{j,j}\\
&\quad - \mathbf{P}\cdot\mathbf{E} - \frac{1}{2}\epsilon_0\epsilon_a((\mathbf{a}\cos\theta + \mathbf{c}\sin\theta)\cdot\mathbf{E})^2. \qquad (2.27)
\end{aligned}$$

Minimizing the energy in (2.27) using the Euler-Lagrange equations the dynamic equation is obtained.

Thus

$$\left(\frac{\partial \mathbf{W}}{\partial a_{i,j}}\right)_{,j} - \frac{\partial \mathbf{W}}{\partial a_i} + g_i^a + \lambda a_i + \mu c_i + e_{ijk}\beta_{k,j} = 0, \qquad (2.28)$$

and

$$\left(\frac{\partial \mathbf{W}}{\partial c_{i,j}}\right)_{,j} - \frac{\partial \mathbf{W}}{\partial c_i} + g_i^c + \chi c_i + \mu a_i = 0, \qquad (2.29)$$

for $i = 1,2,3$, where $a_{i,j}$ represents the partial derivative of the ith component of $\mathbf{a}$ with respect to the jth variable.

Here

$$g_i^a = -2\tau_5\frac{\partial c_i}{\partial t}, \qquad (2.30)$$

$$g_i^c = -2\lambda_5\frac{\partial c_i}{\partial t}, \qquad (2.31)$$

where τ_5 and λ_5 are viscosity coefficients, and λ_5 is a positive rotational viscosity related to the director $\mathbf{n}$ around the fictitious cone [10]. Substituting g_i^a and g_i^c into (2.28) and (2.29) respectively, either evaluates or eliminates the Lagrange multipliers, in order to obtain the equation that governs the

movement of the c-director [9]. Here only (2.29) will be taken into consideration.

Therefore

$$\begin{aligned}\frac{\partial \mathbf{W}}{\partial c_{r,s}} &= 2(B_2 - B_3)c_{i,i}\delta_{r,s} + \frac{1}{2}(B_1 - B_3)[c_s c_{r,k} c_k + c_{r,j} c_j c_s] + B_3 c_{r,s} \\ &\quad + B_{13}[c_s c_{r,k} a_k + c_{r,j} c_j a_s] + (C_1 + C_2) c_j a_{j,k} c_k \delta_{r,s} + C_2 a_{i,i} \delta_{r,s}.\end{aligned}$$

Note: Since $\mathbf{a} = (0, 0, 1)$ differentiating $\mathbf{a}$ with respect to i, j or k will result in zero. Hence for simplicity all the terms which contain $\mathbf{a}$ are set equal to zero.

Thus

$$\begin{aligned}\left(\frac{\partial \mathbf{W}}{\partial c_{r,s}}\right), s &= 2(B_2 - B_3)c_{i,ir} \\ &\quad + \frac{1}{2}(B_1 - B_3)[c_{s,s} c_{r,k} c_k + c_s c_{r,ks} c_k + c_s c_{r,k} c_{k,s} \\ &\quad + c_{r,js} c_j c_s + c_{r,j} c_{j,s} c_s + c_{r,j} c_j c_{s,s}] + B_3 c_{r,ss} \\ &\quad + B_{13}[c_{s,s} c_{r,k} a_k + c_s c_{r,ks} a_k + c_r, jsc_j a_s + c_{r,j} c_{j,s} a_s].\end{aligned}$$

Now set r=1 and sum over the other dummy indices.

Recall

- If $i = j$: $\delta_{i,j} = 1$ and if $i \neq j$: $\delta_{i,j} = 0$,
- $\mathbf{a} = (0, 0, 1)$,
- $\mathbf{b} = (-\sin\phi(x,t), \cos\phi(x,t), 0)$,
- $\mathbf{c} = (\cos\phi(x,t), \sin\phi(x,t), 0)$.

After simplifying, only one nonzero term remains, i.e.

$$\left(\frac{\partial \mathbf{W}}{\partial c_{1,s}}\right), s = B_3 c_{1,33}. \tag{2.32}$$

Similarly when $r = 2$

$$\left(\frac{\partial \mathbf{W}}{\partial c_{2,s}}\right), s = B_3 c_{2,3,3}. \tag{2.33}$$

Now solving for $\dfrac{\partial \mathbf{W}}{\partial c_i}$,

$$\begin{aligned}
\frac{\partial \mathbf{W}}{\partial c_r} &= \frac{1}{2}(B_1 - B_3)\frac{\partial}{\partial c_r}(c_{i,j}c_j c_{i,k}c_k) \\
&\quad + \frac{1}{2}(2A_{11} + A_{12} + A_{21} + B_3 - B_1)\frac{\partial}{\partial c_r}(c_i a_{i,j} c_j)^2 \\
&\quad - \frac{1}{2}(2A_{11} + 2A_{21} + B_3)\frac{\partial}{\partial c_r}(a_{i,i}c_j a_{i,k}c_k) \\
&\quad + B_{13}c_{i,j}c_{i,k}a_k + (C_1 + C_2)\frac{\partial}{\partial c_r}(c_{i,i}c_j a_{j,k}c_k) \\
&\quad - \frac{\partial}{\partial c_r}(P_0 \mathbf{b}\cdot\mathbf{E}) - \epsilon_0\epsilon_a((\mathbf{a}\cos\theta + \mathbf{c}\sin\theta)\cdot\mathbf{E})\cdot(\mathbf{E}\cdot\sin\theta) \\
&= \frac{1}{2}(B_1 - B_3)(c_{i,r}c_{i,k}c_k + c_{i,j}c_j c_{i,r}) \\
&\quad + \frac{1}{2}(2A_{11} + A_{12} + A_{21} + B_3 - B_1)2(c_i a_{i,j}c_j)(a_{r,m}c_m + c_n a_{n,r}) \\
&\quad - \frac{1}{2}(2A_{11} + 2A_{21} + B_3)a_{i,i}(a_{r,k}c_k + c_j a_{j,r}) \\
&\quad + B_{13}c_{i,r}c_{i,k}a_k + (C_1 + C_2)(c_{i,i}a_{r,k}c_k + c_{i,i}c_j a_{j,r}) \\
&\quad - \frac{\partial}{\partial c_r}(P_0 E_0(-\sin\phi, \cos\phi, 0)(\cos\alpha, 0, \sin\alpha)) \\
&\quad + \epsilon_0\epsilon_a E_0(\sin\alpha\cos\theta + \cos\alpha\sin\theta\cos\phi)E_i.
\end{aligned}$$

Note that the last term is derived as shown in [9].

For $r = 1$ and summing over the other dummy indices we obtain,

$$\begin{aligned}
\frac{\partial \mathbf{W}}{\partial c_1} &= -P_0 E_0 \cos\alpha \frac{\partial}{\partial \cos\phi}(1 - \cos^2\phi)^{\frac{1}{2}} \\
&\quad + \epsilon_0\epsilon_a E_0(\cos\phi\sin\theta\cos\alpha + \cos\theta\sin\alpha)\sin\theta E_1 \\
&= -P_0 E_0 \cos\alpha \frac{\cos\phi}{\sin\phi} \\
&\quad + \epsilon_0\epsilon_a E_0^2(\cos\phi\sin\theta\cos\alpha + \cos\theta\sin\alpha)\sin\theta\cos\alpha.
\end{aligned} \tag{2.34}$$

Similarly

$$\frac{\partial \mathbf{W}}{\partial c_2} = 0. \tag{2.35}$$

Equations (2.34) and (2.35) are substituted into the equation that governs the movement of the c-director (2.29).

Since $\mathbf{a}\cdot\mathbf{a} = \mathbf{c}\cdot\mathbf{c} = 1$ and $\mathbf{a}\cdot\mathbf{c} = 0$,

$$a_i \frac{\partial c_i}{\partial t} = 0.$$

Taking the scalar product of

$$\begin{aligned} B_3 c_{i,3,3} - P_0 E_0 \cos\alpha \frac{\cos\phi}{\sin\phi} &+ \epsilon_0 \epsilon_a E_0 (\cos\phi \sin\theta \cos\alpha + \cos\theta \sin\alpha) \sin\theta E_i \\ &- 2\lambda_5 \frac{\partial c_i}{\partial t} + \chi c_i + \mu a_i = 0 \end{aligned} \tag{2.36}$$

with $\mathbf{a}$ we obtain

$$\mu = -\epsilon_0 \epsilon_a E_0^2 (\cos\phi \sin\theta \cos\alpha + \cos\theta \sin\alpha) \sin\theta \sin\alpha. \tag{2.37}$$

For $i = 1$

$$\begin{aligned} B_3 c_{1,3,3} - P_0 E_0 \cos\alpha \frac{\cos\phi}{\sin\phi} &+ \epsilon_0 \epsilon_a E_0^2 (\cos\phi \sin\theta \cos\alpha + \cos\theta \sin\alpha) \sin\theta \cos\alpha \\ &- 2\lambda_5 \frac{\partial c_1}{\partial t} + \chi c_1 + \mu a_1 = 0, \end{aligned} \tag{2.38}$$

becomes

$$\begin{aligned} B_3 c_{1,3,3} - P_0 E_0 \cos\alpha \frac{\cos\phi}{\sin\phi} &+ \epsilon_0 \epsilon_a E_0^2 (\cos\phi \sin\theta \cos\alpha + \cos\theta \sin\alpha) \sin\theta \cos\alpha \\ &- 2\lambda_5 \frac{\partial c_1}{\partial t} + \chi c_1 = 0, \end{aligned} \tag{2.39}$$

which is

$$\begin{aligned} B_3 \left(c_{1,3,3} - c_1 \left(\frac{\partial \phi}{\partial x} \right)^2 \right) &+ -P_0 E_0 \cos\alpha \frac{\cos\phi}{\sin\phi} + \epsilon_0 \epsilon_a E_0^2 \cos\phi \sin^2\theta \cos^2\alpha \\ &+ \epsilon_0 \epsilon_a E_0^2 \cos\theta \sin\alpha \sin\theta \cos\alpha - 2\lambda_5 \frac{\partial c_1}{\partial t} + \chi c_1 = 0. \end{aligned}$$

Substituting for the values $c_{1,3,3}$ and c_1 we obtain,

$$B_3\left(-\cos\phi\left(\frac{\partial\phi}{\partial x}\right)^2-\sin\phi\frac{\partial^2\phi}{\partial x^2}-\cos\phi\left(\frac{\partial\phi}{\partial x}\right)^2\right)+-P_0E_0\cos\alpha\frac{\cos\phi}{\sin\phi}$$
$$+\epsilon_0\epsilon_aE_0^2\cos\phi\sin^2\theta\cos^2\alpha+\epsilon_0\epsilon_aE_0^2\cos\theta\sin\alpha\sin\theta\cos\alpha$$
$$+2\lambda_5\sin\phi\frac{\partial\phi}{\partial t}+\chi\cos\phi=0. \tag{2.40}$$

For $i=2$

$$B_3c_{2,3,3}-2\lambda_5\frac{\partial c_2}{\partial t}+\chi c_2+\mu a_2=0, \tag{2.41}$$

becomes

$$B_3c_{2,3,3}-2\lambda_5\frac{\partial c_2}{\partial t}+\chi c_2=0, \tag{2.42}$$

which is

$$B_3\left(c_{2,3,3}-c_2\left(\frac{\partial\phi}{\partial x}\right)^2\right)-2\lambda_5\frac{\partial c_2}{\partial t}+\chi c_2=0.$$

Substituting for the values $c_{2,3,3}$ and c_2 we obtain,

$$B_3\left(-\sin\phi\left(\frac{\partial\phi}{\partial x}\right)^2+\cos\phi\frac{\partial^2\phi}{\partial x^2}-\sin\phi\left(\frac{\partial\phi}{\partial x}\right)^2\right)$$
$$-2\lambda_5\cos\phi\frac{\partial\phi}{\partial t}+\chi\sin\phi=0. \tag{2.43}$$

Now (2.40) is multiplied by c_2 and (2.43) is multiplied by c_1 and the two are subtracted in order to eliminate χ and to obtain the dynamic equation

$$\begin{aligned}2\lambda_5\frac{\partial\phi}{\partial t} &= B_3\frac{\partial^2\phi}{\partial x^2}-P_0E_0\cos\alpha\cos\phi-\epsilon_0\epsilon_aE_0^2\cos\phi\sin^2\theta\cos^2\alpha\sin\phi\\ &\quad-\epsilon_0\epsilon_aE_0^2\cos\theta\sin\alpha\sin\theta\cos\alpha\sin\phi.\end{aligned} \tag{2.44}$$

2.2 NONDIMENSIONAL DYNAMIC EQUATION

For simplicity, we nondimensionalize the above dynamic equation so that the results can be compared with those already shown.

In [10] it was shown that when the following scaled variables were introduced

$$T = \frac{1}{4} t (2\lambda_5)^{-1} \epsilon_0 \left|\epsilon_a\right| E_0^2 \cos^2 \alpha \sin \theta, \tag{2.45}$$

$$X = \frac{1}{2} x B^{-\frac{1}{2}} (\epsilon_0 \left|\epsilon_a\right| E_0^2 \cos^2 \alpha \sin \theta)^{\frac{1}{2}}, \tag{2.46}$$

where it is assumed that $\epsilon_a < 0$, the dynamic equation can be nondimensionalized to

$$\phi_T = \phi_{XX} + 2d \cos \phi + 4f \sin \phi + 2\phi(2\phi). \tag{2.47}$$

The subscripts denote partial differentiation with respect to the indicated variables and d and f are introduced as dimensionless parameters given by

$$d = 2P_0(\epsilon_0 \epsilon_a E_0 \cos \alpha \sin^2 \theta)^{-1}, \tag{2.48}$$

$$f = \tan \alpha \cot \theta \ll 1. \tag{2.49}$$

Thus

$$\begin{aligned} \tan \alpha &\ll \tan \theta \\ \alpha &\ll \theta + \frac{\pi}{2n}, \end{aligned} \tag{2.50}$$

where $n = 1, 2, \ldots$. This implies that the angle of the electric field to the smectic planes α must be much smaller that the tilt angle θ.

A further transformation

$$u(X, T) = 2\phi(X, T) - \pi, \tag{2.51}$$

results in the nondimensional equation in a standard form [17]

$$u_T = u_{XX} - 4d \sin\left(\frac{u}{2}\right) - 4 \sin u + 8f \cos\left(\frac{u}{2}\right). \tag{2.52}$$

3. LIE POINT SYMMETRIES AND THE STEADY-STATE SOLUTION

Lie point symmetries will be applied to the nondimensional dynamic equation (2.52). An approximate group invariant solution is presented in this section. Results obtained will be compared to those already shown in [10]. Lie point symmetries are appropriate and are used here in order to obtain an approximate analytical solution for our model [18, 19]. We compare these results with those obtained using numerical and pseudo-spectral methods. The steady-state of the nondimensional dynamic equation (2.52), is then obtained. The phase diagrams of the results are then compared with the numerical solutions.

3.1 LIE POINT SYMMETRIES

To solve the nondimensional equation (2.52) by Lie point symmetries, the point transformations are

$$\overline{T} \approx T + g\xi^1(T, X, u) \tag{3.1}$$

$$\overline{X} \approx X + g\xi^2(T, X, u) \tag{3.2}$$

$$\overline{u} \approx u + g\eta(T, X, u). \tag{3.3}$$

These transformations form a group where g is known as the group parameter [20]. The generator of this group is

$$Z = \xi^1(T, X, u)\frac{\partial}{\partial T} + \xi^2(T, X, u)\frac{\partial}{\partial X} + \eta(T, X, u)\frac{\partial}{\partial u}, \tag{3.4}$$

where

$$\xi^1(T, X, u) = \frac{\partial \overline{T}}{\partial g}, \quad \xi^2(T, X, u) = \frac{\partial \overline{X}}{\partial g}, \quad \eta(T, Z, u) = \frac{\partial \overline{u}}{\partial g}, \tag{3.5}$$

and are evaluated at $g = 0$.

ξ^1, ξ^2 and η are calculated by allowing the operator Z to act on (2.52), i.e.

$$Z\left[u_T - u_{XX} + 4d\sin\left(\frac{u}{2}\right) + 4\sin u - 8f\cos\left(\frac{u}{2}\right)\right]\Big|_{(2.52)} = 0. \tag{3.6}$$

Using MATH LIE [21], it then follows that the equation (2.52) admits Lie point symmetries of the form

$$X_1 = \frac{\partial}{\partial T}, \tag{3.7}$$

$$X_2 = \frac{\partial}{\partial X}. \tag{3.8}$$

Hence the nondimensional equation admits travelling wave solutions of the form

$$u(X, T) = F(p), \tag{3.9}$$

$$p = X + vT. \tag{3.10}$$

Substituting these traveling wave solutions (3.9) and (3.10) into the nondimensional equation results in

$$v\frac{dF}{dp} - \frac{d^2F}{dp^2} + 4\left(d\sin\left(\frac{F}{2}\right) + \sin(F) - 2f\cos\left(\frac{F}{2}\right)\right) = 0. \tag{3.11}$$

As in [10] (3.11) admits a Lie point symmetry

$$Y = \frac{\partial}{\partial p}, \tag{3.12}$$

and thus the following substitutions can be made

$$F'(p) = K(F), \tag{3.13}$$

$$F''(p) = K\frac{dK}{dF}. \tag{3.14}$$

The second order differential equation (3.14) then reduces to a first order differential equation

$$K\left(v - \frac{dK}{dF}\right) + 4\left(d\sin\left(\frac{F}{2}\right) + \sin(F) - 2f\cos\left(\frac{F}{2}\right)\right) = 0. \tag{3.15}$$

Equation (3.15) is an Abel equation of the second kind. It admits a particular solution of the form [22]

$$K_0(F) = \pm 4\sin\left(\frac{F}{2}\right), \tag{3.16}$$

$$v = \pm d. \tag{3.17}$$

Perturbation theory is now used to determine an approximate solution of (3.15).

We look for solutions to the first order in ϵ of the form

$$K(F) = K_0(F) + \epsilon K_1(F), \qquad \epsilon \ll 1. \tag{3.18}$$

Substituting (3.18) into (3.15) and setting $f = \epsilon$, we obtain

$$\begin{aligned}(K_0(F) + \epsilon K_1(F))(v - \frac{d}{dF}(K_0(F) + \epsilon K_1(F))) \\ +4\left(d\sin\left(\frac{F}{2}\right) + \sin(F) - 2\epsilon\cos\left(\frac{F}{2}\right)\right) = 0.\end{aligned} \tag{3.19}$$

Separating by coefficients of ϵ the following system is obtained

coefficients of ϵ^0 :

$$K_0(F)\left(v - \frac{dK_0(F)}{dF}\right) + 4\left(d\sin\left(\frac{F}{2}\right) + \sin(F)\right) = 0. \tag{3.20}$$

coefficients of ϵ^1 :

$$K_1(F)v - K_0(F)\frac{dK_1(F)}{dF} - K_1\frac{dK_0(F)}{dF} - 8\cos\left(\frac{F}{2}\right) = 0. \qquad (3.21)$$

Substituting (3.16) and (3.17) into (3.21) one obtains

$$\pm K_1(F)d \pm 4\sin\left(\frac{F}{2}\right)\frac{dK_1(F)}{dF} - K_1\frac{d}{dF}\left(\pm 4\sin\left(\frac{F}{2}\right)\right) - 8\cos\left(\frac{F}{2}\right) = 0. \qquad (3.22)$$

Hence

$$\pm K_1(F)d \pm 4\sin\left(\frac{F}{2}\right)\frac{dK_1(F)}{dF} \pm 2K_1\cos\left(\frac{F}{2}\right) - 8\cos\left(\frac{F}{2}\right) = 0. \qquad (3.23)$$

We can then solve (3.23) as in [10], in terms of an integrating factor, that is

$$\begin{aligned} K_1(F) &= \frac{1}{2}\left(\cos\left(\frac{F}{4}\right)\right)^{-1+\frac{a}{2}}\left(\sin\left(\frac{F}{4}\right)\right)^{-1-\frac{a}{2}} \\ &\quad \left(b_1 \pm \frac{1}{4}\int^F \left(\tan\left(\frac{s}{4}\right)\right)^{\frac{a}{2}}\cos\left(\frac{s}{2}\right)ds\right), \end{aligned} \qquad (3.24)$$

where b_1 is a constant of integration. Since the values for $K_0(F)$ and $K_1(F)$ are known, we can solve for $K(F)$, i.e.

$$K(F) = K_0(F) + \epsilon K_1(F).$$

From (3.13)

$$\begin{aligned} \frac{dF}{dp} &= K_0(F) + \epsilon K_1(F) \\ \frac{dF}{K_0(F) + \epsilon K_1(F)} &= dp \\ \frac{1}{K_0(F)}\left(\frac{1}{1 + \frac{\epsilon K_1(F)}{K_0(F)}}\right)dF &= dp \\ \frac{1}{K_0(F)}\left(1 - \frac{\epsilon K_1(F)}{K_0(F)}\right)dF &= dp. \end{aligned}$$

Now integrate

$$\int \frac{1}{K_0(F)} dF - \epsilon \int \frac{K_1(F)}{K_0^2(F)} dF = p + b_2, \tag{3.25}$$

where b_2 is a constant of integration. Solving this equation in *Mathematica* with

$$\begin{aligned} K_0(F) &= -4 \sin\left(\frac{F}{2}\right), \\ K_1(F) &= \frac{1}{2}\left(\cos\left(\frac{F}{4}\right)\right)^{-1+\frac{d}{2}} \left(\sin\left(\frac{F}{4}\right)\right)^{-1-\frac{d}{2}} \\ &\quad \left(b_1 - \frac{1}{4}\int^F \left(\tan\left(\frac{s}{4}\right)\right)^{\frac{d}{2}} \cos\left(\frac{s}{2}\right) ds\right), \end{aligned}$$

yields

$$\begin{aligned} b_2 + p &= -\frac{1}{2}\log\left(\tan\left(\frac{F}{4}\right)\right) - \epsilon\left(\frac{1}{120}\cos\left(\frac{s}{2}\right)\cot\left(\frac{F}{4}\right)\right. \\ &\quad + \frac{1}{240}\cos\left(\frac{s}{2}\right)\cot\left(\frac{F}{4}\right)\csc\left(\frac{F}{4}\right)^2 - \frac{1}{320}\cos\left(\frac{s}{2}\right)\cot\left(\frac{F}{4}\right)\csc\left(\frac{F}{4}\right)^4 \\ &\quad - \frac{1}{20}\cot\left(\frac{F}{4}\right)\log\left(\cos\left(\frac{s}{4}\right)\right) - \frac{1}{40}\cot\left(\frac{F}{4}\right)\csc\left(\frac{F}{4}\right)^2\log\left(\cos\left(\frac{s}{4}\right)\right) \\ &\quad - \frac{3}{160}\cot\left(\frac{F}{4}\right)\csc\left(\frac{F}{4}\right)^4\log\left(\cos\left(\frac{s}{4}\right)\right) - \frac{1}{120}\cot\left(\frac{F}{4}\right)\sec\left(\frac{s}{4}\right)^2 \\ &\quad \left. - \frac{1}{240}\cot\left(\frac{F}{4}\right)\csc\left(\frac{F}{4}\right)^2\sec\left(\frac{s}{4}\right)^2 - \frac{1}{320}\cot\left(\frac{F}{4}\right)\csc\left(\frac{F}{4}\right)^2\sec\left(\frac{s}{4}\right)^2\right). \end{aligned} \tag{3.26}$$

This solution for $u(X,T) = F(p)$ is in implicit form where s is a constant of integration. When certain values for the constants are given the results in Fig. 3.1 are obtained. These results were also obtained in [10].

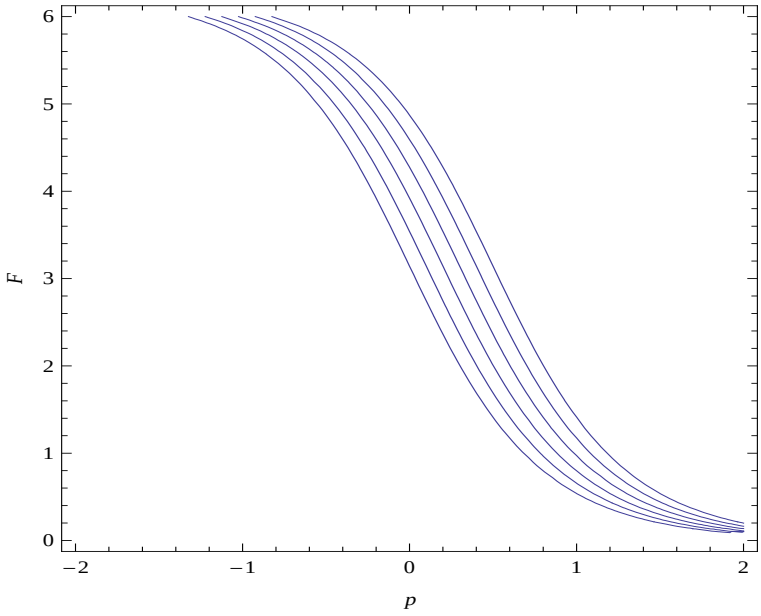

Fig. 3.1: Approximate solutions of the nondimensional dynamic equation (2.52) using Lie point symmetries setting $d = 1$ and $s > 1$. The value for $f = \epsilon$ ranges from 0.0125 to 0.0625 and b_2 ranges from 0.1 to 0.5. These special cases arise from the general solution of (3.26) when $b_2 = 0$ and $v = d$.

3.2 STEADY-STATE SOLUTION

When solving the steady-state system of the dynamic equation, set $u_T = 0$. Thus the following equation is solved

$$u_{XX} = 4d \sin\left(\frac{u(X)}{2}\right) + 4 \sin u(X) - 8f \cos\left(\frac{u(X)}{2}\right).$$

Let

$$\frac{du(X)}{dX} = F(u(X)),$$

then

$$\Rightarrow \frac{d^2u(X)}{dX^2} = F'(u(X))F(u(X)),$$

so that

$$F(u(X))F'(u(X)) = 4d\sin\left(\frac{u(X)}{2}\right) + 4\sin u(X) - 8f\cos\left(\frac{u(X)}{2}\right).$$

Now integrate to obtain

$$\frac{F^2(u(X))}{2} = -8d\cos\left(\frac{u(X)}{2}\right) - 4\sin u(X) - 16f\sin\left(\frac{u(X)}{2}\right) + C,$$

where C is a constant of integration.

Hence

$$F^2(u(X)) = 2\left(-8d\cos\left(\frac{u(X)}{2}\right) - 4\sin u(X) - 16f\sin\left(\frac{u(X)}{2}\right) + C\right)$$

so that

$$F(u(X)) = \pm\sqrt{2\left(-8d\cos\left(\frac{u(X)}{2}\right) - 4\sin u(X) - 16f\sin\left(\frac{u(X)}{2}\right) + C\right)}. \tag{3.27}$$

There are two steady-state solutions depending on which sign is considered in (3.27).

As C increases, the magnitude of $\dfrac{du}{dx}$ increases, with this having no effect on u, i.e. the diameter as shown in Fig. 3.2 remains constant.

Equation (3.27) was then solved numerically in *Mathematica* (see Fig. 3.3).

In order to obtain a steady-state solution, one has to consider the system after a very long time period, i.e. a large time solution is required. In our model two steady-state solutions exist that relate to the numerical solutions obtained in section 5.

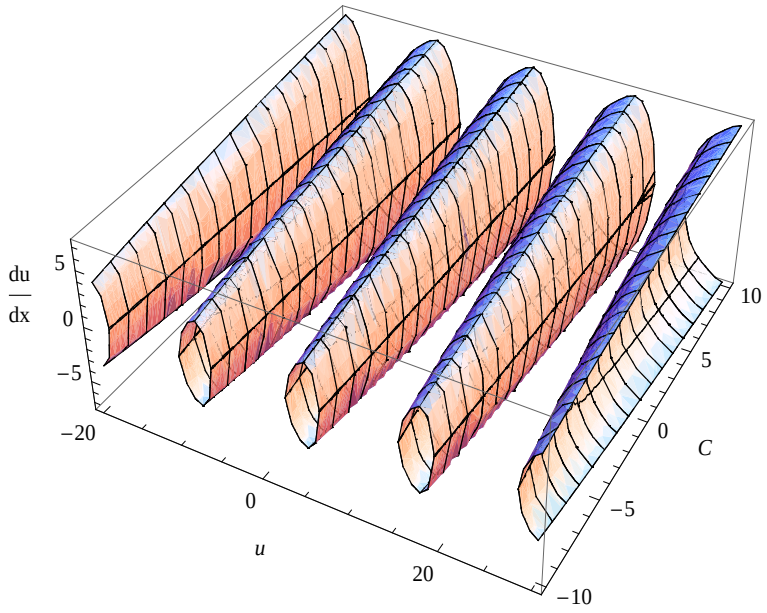

Fig. 3.2: Numerical solution of (3.27) using *Mathematica*

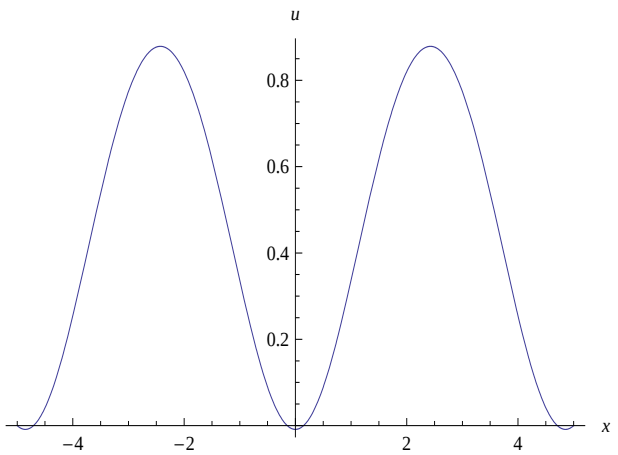

Fig. 3.3: Solution of the ordinary differential equation (3.27) which was solved numerically in *Mathematica*.

4. PSEUDO-SPECTRAL METHODS

The nondimensional dynamic equation (2.52) is solved using pseudo-spectral methods, namely Sinc and Fourier methods. In this section a brief outline is given on how these methods are implemented.

Pseudo-spectral methods are often used to solve partial differential equations. The idea behind these methods is to approximate any function by polynomials. A function u will be approximated by $\widehat{u} = \sum_{n=0}^{N} \widehat{u}_n \phi_n$ where ϕ_n are global polynomials (normally Legendre or Chebychev polynomials) which are called trial functions [23]. Pseudo-spectral methods are more accurate compared to finite difference schemes in terms of stability and convergence. The advantage of pseudo-spectral methods is that they are known to have excellent error properties, and are extremely accurate with a reasonable amount of computation [24].

We will apply two pseudo-spectral methods namely Sinc and Fourier methods. Refer also to [25, 26, 27] to see how pseudo-spectral methods are applied.

4.1 THE SINC METHOD

The Sinc method is a recent technique for solving differential equations and boundary value problems. This method is mainly suited to problems with singular solutions [28]. Works [29, 30] include the use of the Sinc method. A brief outline of the Sinc method is [29, 31]:

- The space variable is discretized into a suitable collocation I_x where $i = 1, ..., n : I_x = \{x_1 = 0, ..., x_i, ..., x_n = 1\}$ and $x_i = (i-1)h$ with $h = \dfrac{1}{n-1}$
- Work in the interval $(-\infty, \infty)$
- The weight function is $\alpha(x) = 1$
- Consider a dependent variable $u = u(t, x)$ which is interpolated and approximated by the values $u_i(t) = u(t, x_i)$ by means of Sinc functions as follows:

$$u(t,x) \cong u^n(t,x) = \sum_{j=1}^{n} S_j(x,h)u_j(t) \tag{4.1}$$

where $u_i(t) = u(t, x_i)$ and

$$S_j(x,h) = \frac{\sin((\frac{\pi}{h})(x-jh))}{\frac{\pi}{h}(x-jh)} \tag{4.2}$$

- This interpolation step can be used to approximate the partial derivatives of the variable u in the nodal points of the discretization

$$\frac{\partial^2 u}{\partial x^2}(t;x_i) \cong \sum_{j=1}^{n} \frac{d^2 S_j}{dx^2}(x_i)u_j(t) = \sum_{j=1}^{n} a_{ji}^{(2)}u_j(t). \tag{4.3}$$

From [29] we have

$$a_{ji}^{(2)} = \frac{2(-1)^{i-j+1}}{h^2(i-j)^2} \tag{4.4}$$

$$a_{ii}^{(2)} = -\frac{1}{3}(\frac{\pi}{h})^2, \tag{4.5}$$

so that the following derivative matrix is obtained

$$D^{(2)} = \frac{1}{h^2}\begin{pmatrix} -\frac{\pi^2}{3} & 2 & -\frac{1}{2} & \dots & \dots & \dots & \frac{2(-1)^n}{(n-1)^2} \\ 2 & -\frac{\pi^2}{3} & 2 & \dots & \dots & \dots & \\ -\frac{1}{2} & 2 & -\frac{\pi^2}{3} & \dots & \dots & \dots & -\frac{1}{2} \\ \vdots & & \ddots & \ddots & & & \vdots \\ \vdots & & & \ddots & \ddots & \ddots & \vdots \\ \frac{2(-1)^{(n-1)}}{(n-2)^2} & \dots & & \dots & \dots & -\frac{\pi^2}{3} & 2 \\ \frac{2(-1)^n}{(n-1)^2} & \dots & \dots & \dots & -\frac{1}{2} & 2 & -\frac{\pi^2}{3} \end{pmatrix}.$$

4.2 THE FOURIER METHOD

This pseudo-spectral method uses Fourier interpolation polynomials to approximate a function. There is no approximation of the spatial derivative, and therefore only a small number of grid points is required for computational accuracy. This reduces computation by a large extent compared to other methods such as finite difference approximations. References [32, 33] use the Fourier method. The Fourier series of a general function $f(x)$ is [34]

$$f(x) = a_0 + \sum_{n=1}^{\infty} a_n \cos(nx) + \sum_{n=1}^{\infty} b_n \sin(nx) \tag{4.6}$$

where

$$a_0 = \frac{1}{2\pi}\int_{-\pi}^{\pi} f(x)dx \tag{4.7}$$

$$a_n = \frac{1}{\pi}\int_{-\pi}^{\pi} f(x)\cos(nx)dx \tag{4.8}$$

$$b_n = \frac{1}{\pi}\int_{-\pi}^{\pi} f(x)\sin(nx)dx \tag{4.9}$$

A brief outline of this method is [31]:

- Work in the interval $[0, 2\pi]$
- The weight function is $\alpha(x) = 1$
- The nodes are computed by $x_k = (k-1)h$ where $h = \frac{2\pi}{N}$ and $k = 1, ..., N$
- Interpolation is as follows:

$$t_N(x) = \sum_{j=1}^{N} \phi_j(x) f_j \tag{4.10}$$

$$\phi_j(x) = \frac{1}{N}\sin\frac{N}{2}(x - x_j)\cot\frac{1}{2}(x - x_j) \tag{4.11}$$

  for N even and

$$\phi_j(x) = \frac{1}{N}\sin\frac{N}{2}(x - x_j)\csc\frac{1}{2}(x - x_j) \tag{4.12}$$

  for N odd.

- The differentiation matrices are calculated as follows

  * For N even: $k, j = 1, ..., N$:

    when $k = j$

$$D_{kj}^{(1)} = 0 \tag{4.13}$$

$$D_{kj}^{(2)} = -\frac{\pi^2}{3h^2} - \frac{1}{6} \tag{4.14}$$

when $k \neq j$

$$D_{kj}^{(1)} = \frac{1}{2}(-1)^{k-j} \cot \frac{(k-j)h}{2} \tag{4.15}$$

$$D_{kj}^{(2)} = -(-1)^{k-j} \frac{1}{2} \csc^2 \frac{(k-j)h}{2} \tag{4.16}$$

* For N odd: $k, j = 1, ..., N$:

  when $k = j$

$$D_{kj}^{(1)} = 0 \tag{4.17}$$

$$D_{kj}^{(2)} = -\frac{\pi^2}{3h^2} - \frac{1}{12} \tag{4.18}$$

  when $k \neq j$

$$D_{kj}^{(1)} = \frac{1}{2}(-1)^{k-j} \csc \frac{(k-j)h}{2} \tag{4.19}$$

$$D_{kj}^{(2)} = -(-1)^{k-j} \frac{1}{2} \csc^2 \frac{(k-j)h}{2} \cot \frac{(k-j)h}{2} \tag{4.20}$$

Note that:

- If N is odd then

$$D^{(l)} = (D^{(l)})^{(l)}. \tag{4.21}$$

- If N is even this only holds for l being odd.

This operator is generated by taking (l) derivatives.

These methods will later be applied to the nondimensional model (2.52) and results will then compared with other numerical techniques.

5. NUMERICAL SOLUTIONS

In this section numerical techniques such as a finite difference approximation, the method of lines, the Sinc method and the Fourier method are applied to the nondimensional dynamic equation (2.52) when which was derived in section 2. The results are then analyzed and discussed.

In [36] it was shown that provided the solution is smooth, pseudo-spectral methods are more accurate compared to finite difference schemes. The disadvantage is that pseudo-spectral methods require more computation for discrete grid models when applied to the same model. We now investigate whether this is also true for the nondimensional dynamic equation (2.52).

The nondimensional equation (2.52) is now solved numerically using methods such as a finite difference approximation, the methods of lines, the Sinc method and the Fourier method. The different methods are applied under the same conditions in order for comparisons to be made. The boundary conditions which will be implemented were chosen according to the analytical solution found in [10], namely

$$u(-\infty, t) = u(\infty, t) = 0. \tag{5.1}$$

Using a finite difference approximation a nonlinear system of ordinary

differential equations is obtained which is solved numerically using ode15s in MATLAB. Since we are dealing with a stiff system, odes15s is used. Sinc and Fourier methods produce a nonlinear dense differentiation matrix. The package, *a MATLAB Differentiation Matrix Suite* [31], is used to calculate these matrices.

5.1 A FINITE DIFFERENCE APPROXIMATION

A finite difference approximation is one of the simplest methods used in numerical analysis. The derivatives which appear in either the ordinary or partial differential equations are approximated by finite differences.

The nondimensional dynamic equation (2.52) is now solved by a finite difference approximation.

Using a forward difference approximation for the time derivative and a central difference approximation for the spatial derivative, (2.52) becomes

$$\begin{aligned}\frac{u_{i,j+1}-u_{i,j}}{\Delta T} &= \left(\frac{u_{i+1,j}-2u_{i,j}+u_{i-1,j}}{(\Delta X)^2}\right)\\ &\quad -4d\sin\left(\frac{u_{i,j}}{2}\right)-4\sin u_{i,j}+8f\cos\left(\frac{u_{i,j}}{2}\right),\end{aligned}$$

so that

$$\begin{aligned}u_{i,j+1}-u_{i,j} &= \frac{\Delta T}{(\Delta X)^2}(u_{i+1,j}-2u_{i,j}+u_{i-1,j})-4d\Delta T\sin\left(\frac{u_{i,j}}{2}\right)\\ &\quad -4\Delta T\sin u_{i,j}+8f\Delta T\cos\left(\frac{u_{i,j}}{2}\right).\end{aligned} \tag{5.2}$$

Now let

$$\kappa = \frac{\Delta T}{2\lambda_5(\Delta X)^2}, \tag{5.3}$$

$$\overline{A} = 4d\Delta T, \tag{5.4}$$

$$\overline{B} = 4\Delta T, \tag{5.5}$$

$$\overline{C} = 8f\Delta T. \tag{5.6}$$

Boundary conditions are

$$u_{0,j} = 0, \tag{5.7}$$

$$u_{n,j} = 0, \tag{5.8}$$

for all values of j. The following system of equations is obtained

$$\begin{bmatrix} u_{0,j+1} \\ u_{1,j+1} \\ u_{2,j+1} \\ \vdots \\ \vdots \\ u_{n-1,j+1} \\ u_{n,j+1} \end{bmatrix} = \begin{bmatrix} 0 & 0 & 0 & ... & ... & ... & 0 \\ \kappa & (1-2\kappa) & \kappa & 0 & ... & \vdots & 0 \\ 0 & \kappa & (1-2\kappa) & \kappa & ... & \vdots & 0 \\ \vdots & \vdots & \vdots & ... & \vdots & \vdots & \vdots \\ \vdots & \vdots & \vdots & ... & \vdots & \vdots & \vdots \\ 0 & 0 & \vdots & ... & \kappa & (1-2\kappa) & \kappa \\ 0 & 0 & ... & ... & ... & 0 & 0 \end{bmatrix} \begin{bmatrix} u_{0,j} \\ u_{1,j} \\ u_{2,j} \\ \vdots \\ \vdots \\ u_{n-1,j} \\ u_{n,j} \end{bmatrix} - \overline{A} \begin{bmatrix} \sin\left(\frac{u_{0,j}}{2}\right) \\ \sin\left(\frac{u_{1,j}}{2}\right) \\ \sin\left(\frac{u_{2,j}}{2}\right) \\ \vdots \\ \vdots \\ \sin\left(\frac{u_{n-1,j}}{2}\right) \\ \sin\left(\frac{u_{n,j}}{2}\right) \end{bmatrix}$$

$$-\overline{B} \begin{bmatrix} \sin u_{0,j} \\ \sin u_{1,j} \\ \sin u_{2,j} \\ \vdots \\ \vdots \\ \sin u_{n-1,j} \\ \sin u_{n,j} \end{bmatrix} + \overline{C} \begin{bmatrix} \cos\left(\frac{u_{0,j}}{2}\right) \\ \cos\left(\frac{u_{1,j}}{2}\right) \\ \cos\left(\frac{u_{2,j}}{2}\right) \\ \vdots \\ \vdots \\ \cos\left(\frac{u_{n-1,j}}{2}\right) \\ \cos\left(\frac{u_{n,j}}{2}\right) \end{bmatrix} - P,$$

where $P = \begin{bmatrix} \overline{C}\cos\left(\frac{u_{0,j}}{2}\right) \\ 0 \\ 0 \\ \vdots \\ \vdots \\ 0 \\ \overline{C}\cos\left(\frac{u_{n,j}}{2}\right) \end{bmatrix}$.

P is included to accommodate for the boundary conditions. This is the only necessary term since $\sin 0 = 0$.

Solving this system in MATLAB the graphical solution as shown in Fig. 5.1 was obtained. From the graph it can be seen that a finite difference approximation results in erratic behaviour at the boundaries and no stable solution is reached. Since this method is unable to produce a smooth solution for our model we look at the method of lines and pseudo-spectral methods for more reliable and stable results.

5.2 THE METHOD OF LINES

The method of lines (MOL) is a numerical technique used to solve partial differential equations where all but one of the dimensions are discretized. This necessitates a system of ordinary differential equations (linear or nonlinear) to be solved. The remaining dimension is solved using analytical solutions, hence it is a combination of analysis and computation. Advantages of the MOL include computational efficiency, numerical stability, less programming effort and less computational time [35].

The MOL is now applied to our nondimensional model (2.52).

The second order derivative in the nondimensional dynamic equation is approximated using a central difference approximation

$$u_{XX} = \frac{u_{i+1}(T) - 2u_i(T) + u_{i-1}(T)}{h^2} \tag{5.9}$$

so that

$$\begin{aligned} u'(T) = & \frac{1}{h^2}\left(u_{i+1}(T) - 2u_i(T) + u_{i-1}(T)\right) \\ & -4d\sin\left(\frac{u_i(T)}{2}\right) - 4\sin u_i(T) + 8f\cos\left(\frac{u_i(T)}{2}\right). \end{aligned} \tag{5.10}$$

Implementing boundary conditions

$$u_0(T) = 0, \tag{5.11}$$

$$u_n(T) = 0, \tag{5.12}$$

we obtain the system of ordinary differential equations

$$
\begin{bmatrix} u_0'(T) \\ u_1'(T) \\ u_2'(T) \\ \vdots \\ \vdots \\ u_{n-1}'(T) \\ u_n'(T) \end{bmatrix} = \frac{1}{h^2} \begin{bmatrix} 0 & 0 & 0 & ... & ... & ... & 0 \\ 1 & -2 & 1 & ... & ... & 0 & \\ 0 & 1 & -2 & 1 & ... & ... & 0 \\ \vdots & & \ddots & \ddots & & & \vdots \\ \vdots & & & \ddots & \ddots & \ddots & \vdots \\ 0 & ... & & ... & ... & 1 & -2 \\ 0 & ... & ... & ... & 0 & 0 & 0 \end{bmatrix} \begin{bmatrix} u_0(T) \\ u_1(T) \\ u_2(T) \\ \vdots \\ \vdots \\ u_{n-1}(T) \\ u_n(T) \end{bmatrix} - 4d \begin{bmatrix} \sin\frac{u_0(T)}{2} \\ \sin\frac{u_1(T)}{2} \\ \sin\frac{u_2(T)}{2} \\ \vdots \\ \vdots \\ \sin\frac{u_{n-1}(T)}{2} \\ \sin\frac{u_n(T)}{2} \end{bmatrix} - 4 \begin{bmatrix} \sin u_0(T) \\ \sin u_1(T) \\ \sin u_2(T) \\ \vdots \\ \vdots \\ \sin u_{n-1}(T) \\ \sin u_n(T) \end{bmatrix}
$$

$$
+8f \begin{bmatrix} \cos\frac{u_0(T)}{2} \\ \cos\frac{u_1(T)}{2} \\ \cos\frac{u_2(T)}{2} \\ \vdots \\ \vdots \\ \cos\frac{u_{n-1}(T)}{2} \\ \cos\frac{u_n(T)}{2} \end{bmatrix} - \begin{bmatrix} 8f\cos\frac{u_0(T)}{2} \\ 0 \\ 0 \\ \vdots \\ \vdots \\ 0 \\ 8f\cos\frac{u_n(T)}{2} \end{bmatrix}.
$$

Solving this system of ordinary differential equations in MATLAB produced the results shown in Fig. 5.2 and Fig. 5.3 for different final times t. The polarization $\mathbf{P}$ affects the numerics of the problem. Without $\mathbf{P}$ the system reaches a potential well (see Fig. 5.4). These results were compared with those obtained in [37] in which films were described and a similar graph was obtained.

5.3 THE SINC METHOD

The Sinc method is now implemented.
Including the boundary conditions

$$u_1(T) = 0, \tag{5.13}$$

$$u_n(T) = 0, \tag{5.14}$$

leads to the system of ordinary differential equations

$$
\begin{bmatrix} u_1'(T) \\ u_2'(T) \\ \vdots \\ \vdots \\ \vdots \\ u_{n-1}'(T) \\ u_n'(T) \end{bmatrix} = \kappa \begin{bmatrix} 0 & 0 & 0 & \dots & \dots & \dots & 0 \\ 2 & -\frac{\pi^2}{3} & 2 & \dots & \dots & \dots & \\ -\frac{1}{2} & 2 & -\frac{\pi^2}{3} & \dots & \dots & \dots & -\frac{1}{2} \\ \vdots & & \ddots & \ddots & & & \vdots \\ \vdots & & & \ddots & \ddots & \ddots & \vdots \\ \frac{2(-1)^{(n-1)}}{(n-2)^2} & \dots & & \dots & \dots & -\frac{\pi^2}{3} & 2 \\ 0 & \dots & \dots & \dots & 0 & 0 & 0 \end{bmatrix} \begin{bmatrix} u_1(T) \\ u_2(T) \\ \vdots \\ \vdots \\ \vdots \\ u_{n-1}(T) \\ u_n(T) \end{bmatrix} - \overline{A} \begin{bmatrix} \sin\left(\frac{u_1(T)}{2}\right) \\ \sin\left(\frac{u_2(T)}{2}\right) \\ \vdots \\ \vdots \\ \vdots \\ \sin\left(\frac{u_{n-1}(T)}{2}\right) \\ \sin\left(\frac{u_n(T)}{2}\right) \end{bmatrix}
$$

$$
-\overline{B} \begin{bmatrix} \sin u_1(T) \\ \sin u_2(T) \\ \vdots \\ \vdots \\ \vdots \\ \sin u_{n-1}(T) \\ \sin u_n(T) \end{bmatrix} + \overline{C} \begin{bmatrix} \cos\left(\frac{u_1(T)}{2}\right) \\ \cos\left(\frac{u_2(T)}{2}\right) \\ \vdots \\ \vdots \\ \vdots \\ \cos\left(\frac{u_{n-1}(T)}{2}\right) \\ \cos\left(\frac{u_n(T)}{2}\right) \end{bmatrix} - \begin{bmatrix} 8f\cos\left(\frac{u_1(T)}{2}\right) \\ 0 \\ \vdots \\ \vdots \\ \vdots \\ 0 \\ 8f\cos\left(\frac{u_n(T)}{2}\right) \end{bmatrix},
$$

where

$$\kappa = \frac{1}{h^2}, \overline{A} = 4d, \overline{B} = 4 \text{ and } \overline{C} = 8f.$$

When solving this system at different time intervals the graphical results in Fig. 5.5 and Fig. 5.6 are obtained. From these graphs it can be seen that as time increases the energy of the system reaches a potential hill and once this state is reached, no further increase in time would affect the system.

The polarization **P** affects the numerics of the problem. Without **P** the system reaches a potential well (see Fig. 5.7). These results were compared with those by obtained in [37] in which electrically driven hybrid instabilities in SmC liquid crystal films were described and a similar graph was obtained.

5.4 THE FOURIER METHOD

The differentiation matrix that was obtained in section 4.2 for the Fourier method, is now applied to the nondimensional equation (2.52). Implementing the boundary conditions

$$u_1(T) = 0, \tag{5.15}$$

$$u_n(T) = 0, \tag{5.16}$$

we obtain the following system of ordinary differential equations for N even and N odd respectively:

$$
\begin{bmatrix} u_1'(T) \\ u_2'(T) \\ \vdots \\ \vdots \\ \vdots \\ \vdots \\ u_{n-1}'(T) \\ u_n'(T) \end{bmatrix} = \begin{bmatrix} 0 & 0 & 0 & \cdots & \cdots & \cdots & 0 \\ \frac{1}{2}\csc^2\left(\frac{h}{2}\right) & -\frac{\pi^2}{3h^2}-\frac{1}{6} & \frac{1}{2}\csc^2\left(\frac{h}{2}\right) & \cdots & \cdots & \cdots & \\ -\frac{1}{2}\csc^2(h) & \frac{1}{2}\csc^2\left(\frac{h}{2}\right) & -\frac{\pi^2}{3h^2}-\frac{1}{6} & \frac{1}{2}\csc^2\left(\frac{h}{2}\right) & \cdots & \cdots & \cdots \\ \vdots & & \ddots & \ddots & & & \vdots \\ \vdots & & & \ddots & \ddots & \ddots & \vdots \\ \cdots & \cdots & \cdots & \cdots & \cdots & -\frac{\pi^2}{3h^2}-\frac{1}{6} & \frac{1}{2}\csc^2\left(-\frac{h}{2}\right) \\ 0 & \cdots & \cdots & \cdots & 0 & 0 & 0 \end{bmatrix} \begin{bmatrix} u_1(T) \\ u_2(T) \\ \vdots \\ \vdots \\ \vdots \\ \vdots \\ u_{n-1}(T) \\ u_n(T) \end{bmatrix}
$$

$$
-\overline{A}\begin{bmatrix} \sin\left(\frac{u_1(T)}{2}\right) \\ \sin\left(\frac{u_2(T)}{2}\right) \\ \vdots \\ \vdots \\ \vdots \\ \sin\left(\frac{u_{n-1}(T)}{2}\right) \\ \sin\left(\frac{u_n(T)}{2}\right) \end{bmatrix} - \overline{B}\begin{bmatrix} \sin u_1(T) \\ \sin u_2(T) \\ \vdots \\ \vdots \\ \vdots \\ \sin u_{n-1}(T) \\ \sin u_n(T) \end{bmatrix} + \overline{C}\begin{bmatrix} \cos\left(\frac{u_1(T)}{2}\right) \\ \cos\left(\frac{u_2(T)}{2}\right) \\ \vdots \\ \vdots \\ \vdots \\ \cos\left(\frac{u_{n-1}(T)}{2}\right) \\ \cos\left(\frac{u_n(T)}{2}\right) \end{bmatrix} - \begin{bmatrix} 8f\cos\left(\frac{u_1(T)}{2}\right) \\ 0 \\ \vdots \\ \vdots \\ \vdots \\ 0 \\ 8f\cos\left(\frac{u_n(T)}{2}\right) \end{bmatrix},
$$

$$
\begin{bmatrix} u_1'(T) \\ u_2'(T) \\ \vdots \\ \vdots \\ \vdots \\ \vdots \\ u_{n-1}'(T) \\ u_n'(T) \end{bmatrix} = \kappa \begin{bmatrix} 0 & 0 & 0 & \dots & \dots & \dots & 0 \\ \frac{1}{2}\csc^2\left(\frac{h}{2}\right)\cot\left(\frac{h}{2}\right) & -\left(\frac{\pi^2}{3h^2}\right)-\frac{1}{12} & \dots & \dots & \dots & \dots & \\ \vdots & \frac{1}{2}\csc^2\left(\frac{h}{2}\right)\cot\left(\frac{h}{2}\right) & \dots & \dots & \dots & \dots & \dots \\ \vdots & & \ddots & \ddots & & & \vdots \\ \vdots & & & \ddots & \ddots & \ddots & \vdots \\ \dots & \dots & \dots & \dots & \dots & -\frac{\pi^2}{3h^2}-\frac{1}{12} & \frac{1}{2}\csc^2\left(-\frac{h}{2}\right)\cot\left(-\frac{h}{2}\right) \\ 0 & \dots & \dots & \dots & .. & 0 & 0 \end{bmatrix} \begin{bmatrix} u_1(T) \\ u_2(T) \\ \vdots \\ \vdots \\ \vdots \\ \vdots \\ u_{n-1}(T) \\ u_n(T) \end{bmatrix}
$$

$$
-\overline{A} \begin{bmatrix} \sin\left(\frac{u_1(T)}{2}\right) \\ \sin\left(\frac{u_2(T)}{2}\right) \\ \vdots \\ \vdots \\ \vdots \\ \vdots \\ \sin\left(\frac{u_{n-1}(T)}{2}\right) \\ \sin\left(\frac{u_n(T)}{2}\right) \end{bmatrix} - \overline{B} \begin{bmatrix} \sin u_1(T) \\ \sin u_2(T) \\ \vdots \\ \vdots \\ \vdots \\ \sin u_{n-1}(T) \\ \sin u_n(T) \end{bmatrix} + \overline{C} \begin{bmatrix} \cos\left(\frac{u_1(T)}{2}\right) \\ \cos\left(\frac{u_2(T)}{2}\right) \\ \vdots \\ \vdots \\ \vdots \\ \cos\left(\frac{u_{n-1}(T)}{2}\right) \\ \cos\left(\frac{u_n(T)}{2}\right) \end{bmatrix} - \begin{bmatrix} 8f\cos\left(\frac{u_1(T)}{2}\right) \\ 0 \\ \vdots \\ \vdots \\ \vdots \\ 0 \\ 8f\cos\left(\frac{u_n(T)}{2}\right) \end{bmatrix}.
$$

When solving the above systems at different time intervals, the graphs shown in Fig. 5.8 and Fig. 5.9 were obtained. The polarization **P** affects the numerics of the problem. Without **P** the system reaches a potential well (see Fig. 5.9).

From the results obtained it can be seen that all methods, except a finite difference approximation, will converge to the same solution, however not necessarily at the same rate. Also, polarization **P** has the same affect on all the methods used. These results were compared to those by obtained in [37] in which films were described and a similar graph was obtained. The profiles of each method were recorded in MATLAB. This is discussed in more detail in the following section.

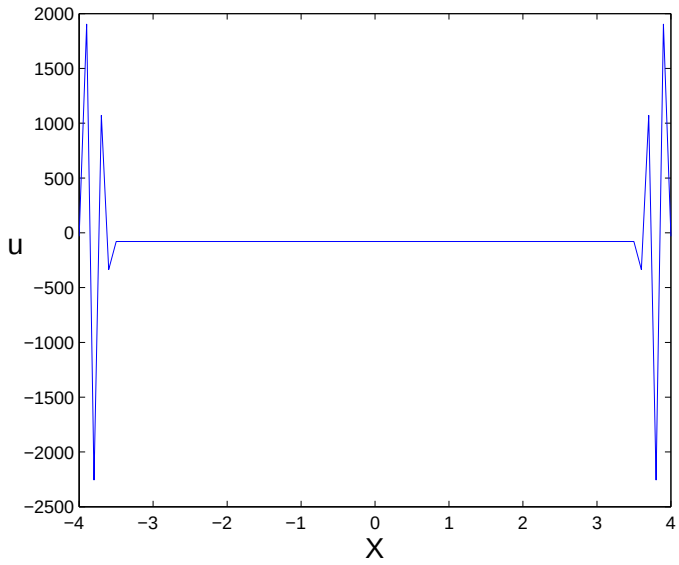

Fig. 5.1: Numerical solution of the nondimensional dynamic model (2.52) shows erratic behaviour occurring at the boundaries. A non-smooth solution is obtained when using a finite difference approximation.

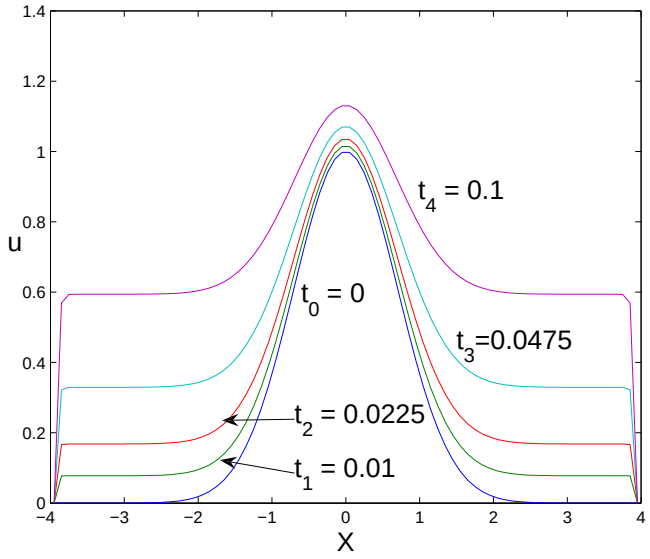

Fig. 5.2: Numerical solution of the nondimensional dynamic model (2.52) using the method of lines with a small final time $t_{final} = 0.1$. The graph shows the rotation angle u is symmetric about the X-axis, and is decreasing with increasing magnitude of X. The boundary conditions at $u_0(T) = 0$ and $u_n(T)$ force the rotation angle to be zero.

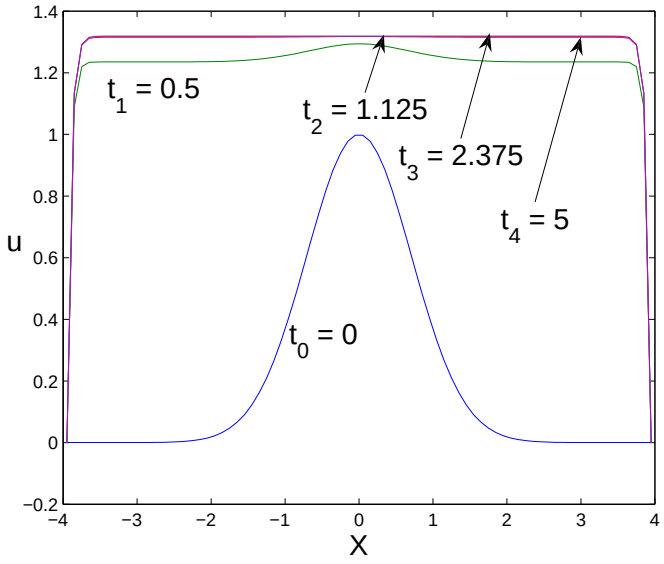

Fig. 5.3: Numerical solution of the nondimensional dynamic model (2.52) using the method of lines with a larger final time $t_{final} = 5$. The graph shows that the rotation angle u is symmetric about the X-axis and over a larger period of time it converges until a potential hill is reached. The boundary conditions at $u_0(T) = 0$ and $u_n(T)$ force u to be zero.

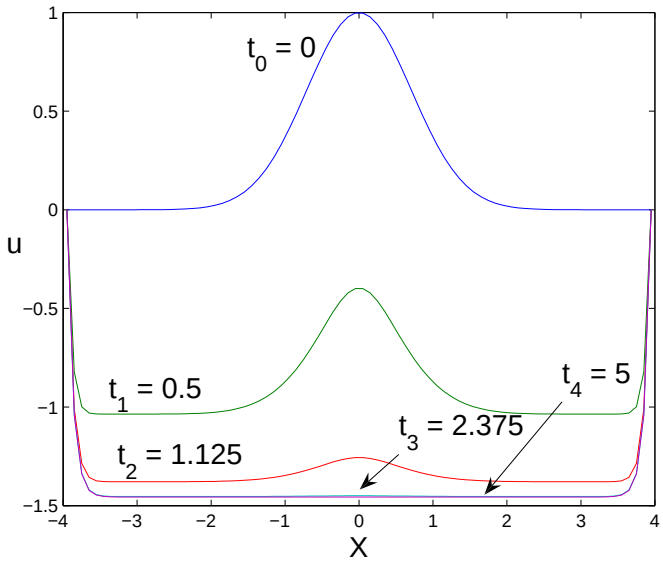

Fig. 5.4: When polarization **P** is absent, the rotation angle u converges to a potential well over a period of time when using the method of lines.

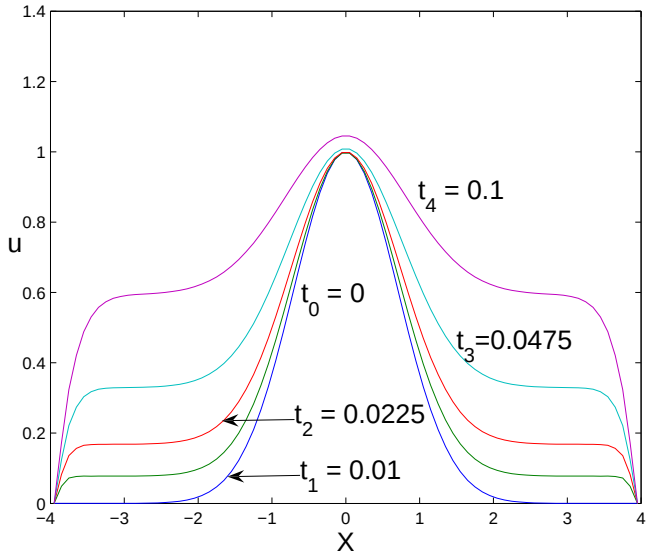

Fig. 5.5: Numerical solution of the nondimensional dynamic model (2.52) using the Sinc method with a small final time $t_{final} = 0.1$. The graph shows the rotation angle u is symmetric about the X-axis, and is decreasing with increasing magnitude of X. The boundary conditions at $u_1(T) = 0$ and $u_n(T)$ force the rotation angle to be zero.

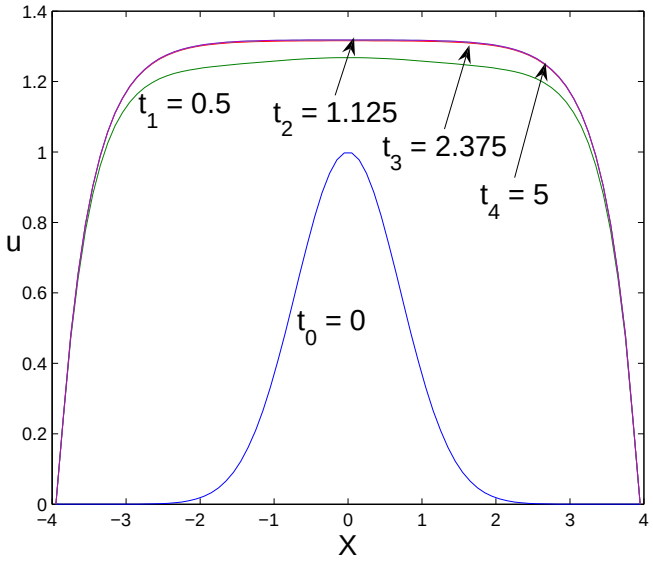

Fig. 5.6: Numerical solution of the nondimensional dynamic model (2.52) using the Sinc method with a larger final time $t_{final} = 5$. The graph shows that the rotation angle u is symmetric about the X-axis and over a larger period of time it converges until a potential hill is reached. The boundary conditions at $u_1(T) = 1$ and $u_n(T)$ force u to be zero.

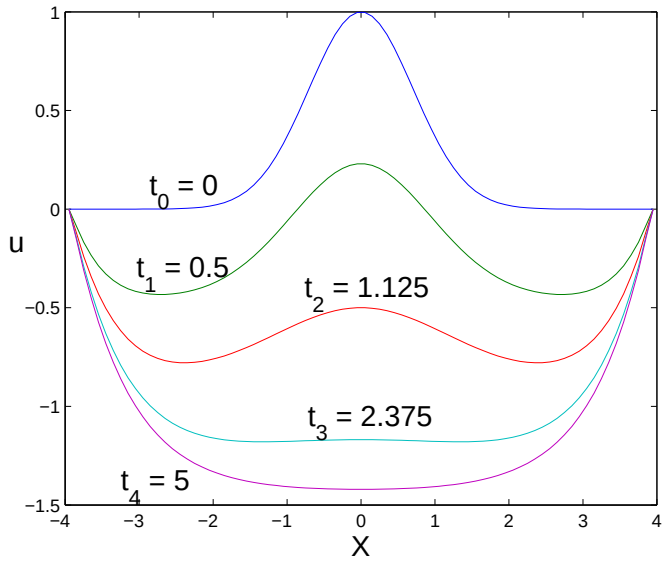

Fig. 5.7: When polarization **P** is absent from the problem, the rotation angle u (over time) converges to a potential well when using the Sinc method.

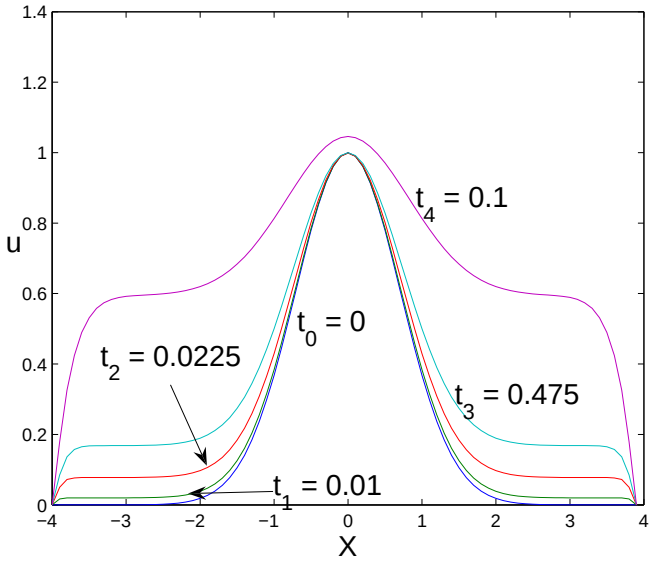

Fig. 5.8: Numerical solution of the nondimensional dynamic model (2.52) using the Fourier method with a small final time $t_{final} = 0.1$. The graph shows the rotation angle u is symmetric about the X-axis, and is decreasing with increasing magnitude of X. The boundary conditions at $u_1(T) = 0$ and $u_n(T)$ force the rotation angle to be zero.

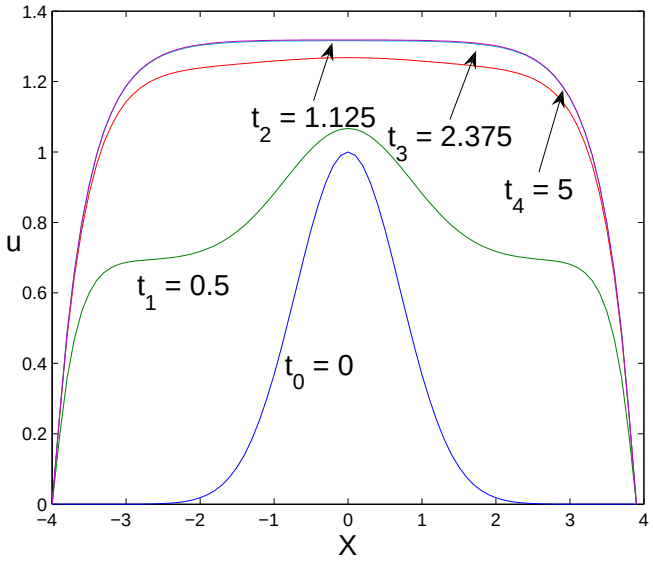

Fig. 5.9: Numerical solution of the nondimensional dynamic model (2.52) using the Fourier method with a larger final time $t_{final} = 5$. The graph shows that the rotation angle u is symmetric about the X-axis and over a larger period of time it converges until a potential hill is reached. The boundary conditions at $u_1(T) = 0$ and $u_n(T)$ force u to be zero.

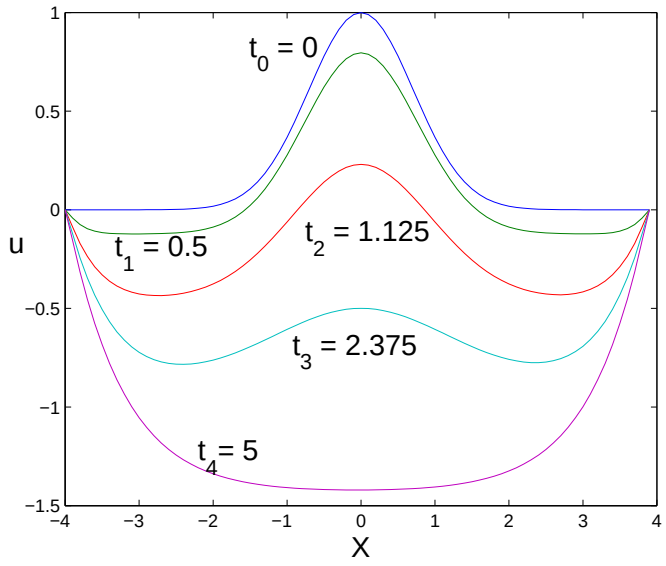

Fig. 5.10: When polarization **P** is absent, the rotation angle u (over time) converges to a potential well when using the Fourier method.

6. CONCLUSION AND FUTURE WORK

For the MOL, Sinc and Fourier methods, it was shown that a stable solution is reached after a period of time and the system will not change with any further increase in t_{final}. The reason is that all the SmC liquid crystals are aligned in a particular position around the fictitious cone and any further time increase will not affect the model. This is very similar to a magnetic field applied to iron filings. When the magnetic field is applied the iron filings become magnetized. They move and all align in the same direction without any further movement until the magnetic field has no further effect. SmC liquid crystals have polarizable substituents and can therefore be easily polarized when an electric current is applied. Across this electric field, the liquid and the crystal properties of the liquid crystal are both being affected. The graphical results obtained in section 5 illustrate this phenomenon. A potential hill, namely a region surrounding a local maximum of potential energy is reached when energy captured here cannot be converted into any other form.

The electric field $\mathbf{E}$ makes a small angle $\alpha > 0$ with the smectic planes. The effect of α on the liquid crystal was also observed; α was set to zero, even integer multiples of π were selected and $t_{final} = 5$. The electric field is parallel to the $X - y$ plane and has a greater effect on the model since

as shown in Fig. 6.1 there is a distinct curvature of the graphs. The value of α was then increased to $\frac{\pi}{2}$ and odd integer multiples of $\frac{\pi}{2}$. From Fig. 6.2 we observe that the electric field now has very little effect on the model since it is perpendicular to the $X - y$ plane. α was increased to π and odd integer multiples of π were selected. The same results were obtained when there was no polarization present in the model (see Fig. 6.3).

For all four methods MATLAB was implemented and profiles of each numerical solution were obtained. Each method was implemented a number of times and the average running time was calculated. The results are shown in Table 6, where all the methods were run with $t_{final} = 0.1$ and the average time it took to run each method was recorded. The same was done for $t_{final} = 5$.

Table 6.1: **Running times of the different methods used in MATLAB**

	$t_{final} = 0.1$	$t_{final} = 5$
Sinc	0.9477	1.0107
Fourier	0.5393	0.6057
The method of lines	0.9177	0.9812

Even though a finite difference approximation is known to be one of the simplest methods applied in numerical analysis, it does not work well for our model. The other three algorithms solve our nondimensional dynamic model (2.52) accurately and efficiently and converge to the steady-state solution obtained in [10], with Fourier method being the most efficient. The Fourier

method decomposes a periodic function into a sum of sines and cosines which oscillate and our model contains these terms.

Future work in this field may include focusing on different smectic liquid crystals, for example smectic-A, smectic-B. One could also consider a varying magnetic field or varying temperature in the system.

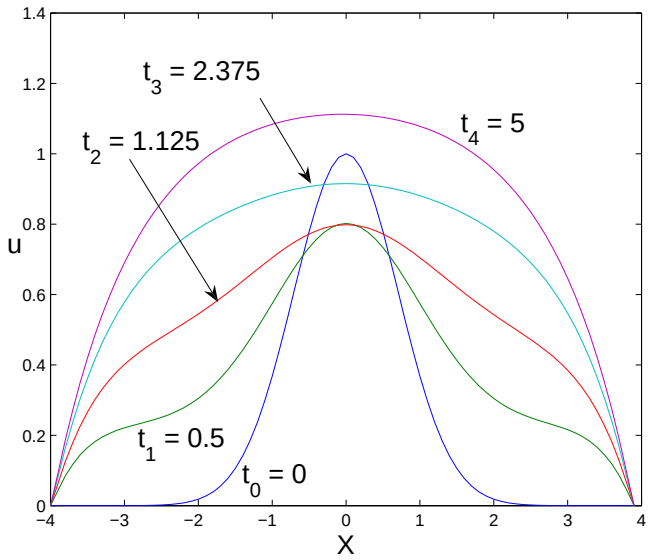

Fig. 6.1: With $\alpha = 0; 2\pi; 4\pi...$, the electric field is parallel to the $X - y$ plane.

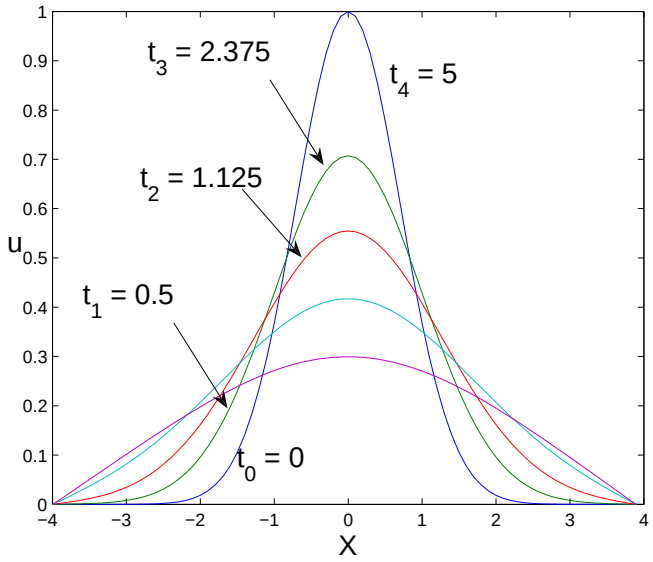

Fig. 6.2: With $\alpha = \frac{\pi}{2}; \frac{3\pi}{2}; \frac{5\pi}{2}...$, the electric field is perpendicular to the $X - y$ plane.

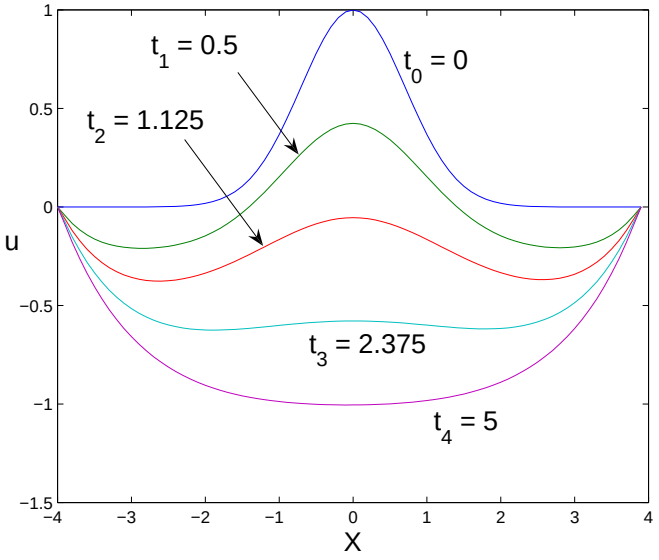

Fig. 6.3: With $\alpha = \pi; 3\pi; 5\pi...$, the electric field is parallel to the $X - y$ plane.

APPENDIX

A.1: For the derivation of the model described in section 2 the following relationships and constraints need to be satisfied.

- $\mathbf{a} \cdot \mathbf{a} = 1, \mathbf{c} \cdot \mathbf{c} = 1, \mathbf{a} \cdot \mathbf{c} = 0, \nabla \times \mathbf{a} = \mathbf{0}.$ (A-1)

Since $\mathbf{a} = (0, 0, 1)$, it follows that

$$\begin{aligned} \mathbf{a} \cdot \mathbf{a} &= (0,0,1) \cdot (0,0,1) \\ &= 0 + 0 + 1 \\ &= 1. \end{aligned} \qquad \square$$

Since $\mathbf{c} = (\cos\phi(x,t), \sin\phi(x,t), 0)$, it follows that

$$\begin{aligned} \mathbf{c} \cdot \mathbf{c} &= (\cos\phi, \sin\phi, 0) \cdot (\cos\phi, \sin\phi, 0) \\ &= \cos^2\phi + \sin^2\phi + 0 \\ &= 1. \end{aligned} \qquad \square$$

Also,

$$\begin{aligned} \mathbf{a} \cdot \mathbf{c} &= (0,0,1) \cdot (\cos\phi, \sin\phi, 0) \\ &= 0 + 0 + 0 \\ &= 0. \end{aligned} \qquad \square$$

For the last constraint it follows that

$$\begin{aligned} \nabla \times \mathbf{a} &= \begin{vmatrix} x & y & z \\ \dfrac{\partial}{\partial x} & \dfrac{\partial}{\partial y} & \dfrac{\partial}{\partial z} \\ 0 & 0 & 1 \end{vmatrix} \\ &= \left(\frac{\partial}{\partial y}(1) - 0; -\frac{\partial}{\partial x}(1) - 0; 0 \right) \\ &= 0. \end{aligned} \qquad \square$$

- The Kronecker delta

$$\delta_{ij} = a_i a_j + b_i b_j + c_i c_j, \tag{A-2}$$

is needed and is proved by first showing that the definition of $a_i a_j$ in tensor form is given by $a_i a_j = e_{irs} e_{jpq} c^r b^s c^p b^q$

where

$$e_{irs} e_{jpq} = \begin{vmatrix} \delta_{ij} & \delta_{ip} & \delta_{iq} \\ \delta_{rj} & \delta_{rp} & \delta_{rq} \\ \delta_{sj} & \delta_{sp} & \delta_{sq} \end{vmatrix}.$$

$$\begin{aligned} a_i a_j &= \delta_{ij}(\delta_{rp}\delta_{sq} - \delta_{sp}\delta_{rq}) c^r b^s c^p b^q + \delta_{ip}(\delta_{rq}\delta_{sj} - \delta_{rj}\delta_{sq}) c^r b^s c^p b^q \\ &\quad + \delta_{iq}(\delta_{rj}\delta_{sp} - \delta_{sj}\delta_{rp}) c^r b^s c^p b^q \\ &= \delta_{ij}[c^p b^q c^p b^q - c^q b^p c^p b^q] + c_i(c^q b^q b_j - c_j b_q b^q) \\ &\quad + b_i(c_j b_p c^p - b_j c^p c^p) \\ &= \delta_{ij} - c_i c_j - b_i b_j. \end{aligned}$$

This implies

$$\delta_{ij} = a_i a_j + b_i b_j + c_i c_j. \qquad \square$$

A.2: Since the vectors **a**, **b** and **c** are orthonormal it follows that

- $a_i a_i = b_i b_i = c_i c_i = 1.$ (A-3)

- $a_i b_i = b_i c_i = c_i a_i = 0.$ (A-4)

Further constraints on **a** imply that

- $a_{i,j} = a_{j,i}.$ (A-5)

Since $\nabla \times \mathbf{a} = 0$, it follows that $\epsilon_{ijk} a_{j,k} = 0$. Thus

$$\begin{aligned} & \epsilon^{ipq}\epsilon_{ijk} a_{j,k} = 0 \\ \Rightarrow \quad & (\delta^p_j \delta^q_k - \delta^p_k \delta^q_j) a_{j,k} = 0 \\ \Rightarrow \quad & a_{p,q} - a_{q,k} = 0 \\ \Rightarrow \quad & a_{i,j} = a_{j,i}. \end{aligned}$$ □

Furthermore we need to show that the following relationships hold

- $a_j a_{j,i} = b_j b_{j,i} = c_j c_{j,i} = 0.$ (A-6)
- $a_j b_{j,i} = -b_j a_{j,i} = -a_{i,j} b_j.$ (A-7)
- $b_j c_{j,i} = -c_j b_{j,i}.$ (A-8)
- $a_j c_{j,i} = -c_j a_{j,i} = -a_{i,j} c_j.$ (A-9)
- $a_i b_{i,j} a_j = a_i c_{i,j} a_j = 0.$ (A-10)

Proving (A-6) is trivial. However in (A-7), since **a** and **b** are orthonormal we have

$$a_j b_j = 0. \tag{A-11}$$

Differentiating (A-11) with respect to i leads to

$$\begin{aligned} a_{j,i} b_j + a_j b_{j,i} &= 0, \\ \Rightarrow a_j b_{j,i} &= -b_j a_{j,i}. \end{aligned}$$

Also

$$b_j a_j = 0. \tag{A-12}$$

Differentiating (A-12) with respect to i leads to

$$\begin{aligned} b_{j,i}a_j + b_j a_{j,i} &= 0, \\ \Rightarrow b_{j,i}a_j &= -b_j a_{j,i}, \end{aligned}$$

and we have $a_{i,j} = a_{j,i}$ as shown previously. Hence

$$a_j b_{j,i} = -a_{i,j}b_j.$$

Therefore,

$$a_j b_{j,i} = -b_j a_{j,i} = -a_{i,j}b_j. \qquad \square$$

We now show that (A-8) and (A-9) are valid. Since **b** and **c** are orthonormal we have

$$b_j c_j = 0. \tag{A-13}$$

Differentiating (A-13) with respect to i leads to

$$\begin{aligned} b_{j,i}c_j + b_j c_{j,i} &= 0 \\ \Rightarrow b_j c_{j,i} &= -c_j b_{j,i}. \end{aligned} \qquad \square$$

Since **a** and **c** are orthonormal we have

$$a_j c_j = 0. \tag{A-14}$$

Differentiating (A-14) with respect to i to obtain

$$\begin{aligned} a_{j,i}c_j + a_j c_{j,i} &= 0, \\ \Rightarrow a_j c_{j,i} &= -c_j a_{j,i}. \end{aligned}$$

Also

$$c_j a_j = 0. \tag{A-15}$$

Differentiate (A-15) with respect to i

$$\begin{aligned} c_{j,i}a_j + c_j a_{j,i} &= 0, \\ c_{j,i}a_j &= -c_j a_{j,i}. \end{aligned}$$

We also have $a_{i,j} = a_{j,i}$ as shown previously. Hence

$$a_j c_{j,i} = -a_{i,j}c_j.$$

Therefore,

$$a_j c_{j,i} = -c_j a_{j,i} = -a_{i,j}c_j. \qquad \square$$

It was previously shown that $a_i b_{i,j} a_j = -a_i b_i a_{i,j}$. This can be written as

$$\begin{aligned} -a_i b_i a_{i,j} &= -a_i a_{i,j} b_i \\ &= 0. \end{aligned}$$

Hence

$$a_i b_{i,j} a_j = 0.$$

Similarly, $a_i c_{i,j} a_j = -a_{j,i} c_j a_j$, which simplifies to

$$a_i c_{i,j} a_j = 0. \qquad \square$$

.

Further identities follow

- $b_i b_j b_k b_p a_{i,j} a_{k,p}$ (A-16)
- $b_i b_j b_k b_p c_{i,j} a_{k,p}$ (A-17)
- $b_i b_j b_k b_p c_{i,j} c_{k,p}$. (A-18)

From the previous equations and [16] b can be eliminated to obtain

$$\begin{aligned} 2a_{i,j}c_j a_{i,k}c_k &= 2a_{i,i}c_j a_{j,k}c_k - S_3, && \text{(A-19)} \\ a_{i,j}c_j c_{i,k}c_k &= c_{i,i}c_j a_{j,k}c_k - S_2, && \text{(A-20)} \\ c_{i,j}a_j c_{i,k}a_k &= c_{i,j} - (c_{i,i})^2 - c_{i,j}c_j c_{i,k}c_k \\ &\quad +(c_i a_{i,j}c_j)^2 - a_{i,j}c_j a_{i,k}c_k, && \text{(A-21)} \\ 2a_{i,j}c_j c_{i,k}a_k &= S_1. && \text{(A-22)} \end{aligned}$$

Similarly,

- $c_i c_j c_k c_p a_{i,j} a_{k,p}$ (A-23)
- $c_i c_j c_k c_p b_{i,j} b_{k,p}$, (A-24)

becomes

$$\begin{aligned} 2a_{i,j}b_j a_{i,k}b_k &= 2a_{i,i}b_j a_{j,k}b_k - S_3, && \text{(A-25)} \\ b_{i,j}a_j b_{i,k}a_k &= b_{i,j}b_{i,j} - (b_{i,i})^2 - b_{i,j}b_j b_{i,k}b_k \\ &\quad +(b_i a_{i,j}b_j)^2 - a_{i,j}b_j a_{i,k}b_k, && \text{(A-26)} \\ 2a_{i,j}b_j b_{i,k}a_k &= S_4, && \text{(A-27)} \end{aligned}$$

where

$$\begin{aligned} S_1 &= (c_i c_{j,j} - c_j c_{i,j})_{,i}, \\ S_2 &= (a_i c_{j,j} - a_j c_{i,j})_{,i}, \\ S_3 &= (a_{i,i})^2 - a_{i,j}a_{i,j}, \\ S_4 &= b_{i,i}b_{j,j} - b_{i,j}b_{j,i}. \end{aligned}$$

Now we can solve for each of the terms in the main equation (2.10).

- $\mathbf{a} \cdot \nabla \times \mathbf{c}$. (A-28)

Written in tensor form $\mathbf{a} \cdot \nabla \times \mathbf{c} = a_i e_{ijk} c_{k,j}$, where

$a_i = e_{imn} c_m b_n$, since $\mathbf{a} = \mathbf{c} \times \mathbf{b}$.

Thus

$$\begin{aligned} \mathbf{a} \cdot \nabla \times \mathbf{c} &= e_{imn} c_m b_n s_{ijk} c_{k,j} \\ &= e_{imn} e_{ijk} c_m b_n c_{k,j} \\ &= c_j b_k c_{k,j} - c_k b_j c_{k,j} \\ &= c_j b_k c_{k,j}. \end{aligned}$$

By using the relationship $b_j c_{j,i} = -c_j b_{j,i}$, which was shown previously.

$$\mathbf{a} \cdot \nabla \times \mathbf{c} = c_j c_k b_{k,j}. \tag{A-29}$$

Before going any further it must be shown that

$$\begin{aligned} \mathbf{a} = \mathbf{c} \times \mathbf{b} \quad &\Rightarrow \quad \nabla \times \mathbf{a} = \nabla \times (\mathbf{c} \times \mathbf{b}) = 0 \\ &\Rightarrow \quad e_{ijk} \frac{\partial}{\partial x^j} (\mathbf{c} \times \mathbf{b})_{,k} = 0 \\ &\Rightarrow \quad e_{ijk} (\mathbf{c} \times \mathbf{b})_{k,j} = 0 \\ &\Rightarrow \quad e_{ijk} e_{kpq} (c_p b_q)_{,j} = 0 \\ &\Rightarrow \quad (\delta_{ip} \delta_{jq} - \delta_{iq} \delta_{jp}) (c_p b_q)_{,j} = 0 \\ &\Rightarrow \quad (c_i b_j)_{,j} - (c_j b_i)_{,j} = 0 \\ &\Rightarrow \quad c_{i,j} b_j + c_i b_{j,j} - cj, j b_i - c_j b_{i,j} = 0. \end{aligned}$$

Since i is a dummy variable we can set it to equal k, i.e.

$$c_{k,j} b_j + c_k b_{j,j} - c_{j,j} b_k - c_j b_{k,j} = 0 \tag{A-30}$$

$$\Rightarrow c_j b_{k,j} = c_{k,j} b_j + c_k b_{j,j} - c_{j,j} b_k. \tag{A-31}$$

We can substitute this into (A-29), thus

$$\begin{aligned} \mathbf{a} \cdot \nabla \times \mathbf{c} &= -c_k[c_{k,j}b_j + c_k b_j, j - c_{j,j}b_k] \\ &= -c_k c_{k,j} b_j - (c_k c_k) b_{j,j} + c_k b_k c_{j,j} \\ &= -b_{j,j}. \end{aligned} \tag{A-32}$$

□

- $\mathbf{b} \cdot \nabla \times \mathbf{c}$. (A-33)

Written in tensor form $\mathbf{b} \cdot \nabla \times \mathbf{c} = b_i e_{ijk} c_{k,j}$, where $b_i = e_{imn} a_m c_n$, since $\mathbf{b} = \mathbf{a} \times \mathbf{c}$.

Thus

$$\begin{aligned} \mathbf{b} \cdot \nabla \times \mathbf{c} &= e_{imn} a_m c_n e_{ijk} c_{k,j} \\ &= e_{imn} e_{ijk} a_m c_n c_{k,j} \\ &= (\delta_{mj}\delta_{nk} - \delta_{mk}\delta_{nj}) a_m c_n c_{k,j} \\ &= a_j c_k c_{k,j} - a_k c_j c_{k,j} \\ &= -a_k c_j c_{k,j}. \end{aligned}$$

From the relationship $a_j c_{j,i} = -c_j a_{j,i}$ which was shown previously, and since k is a dummy variable we can set it equal to i, and obtain

$$\mathbf{b} \cdot \nabla \times \mathbf{c} = c_i a_{i,j} c_j. \tag{A-34}$$

□

- $\mathbf{c} \cdot \nabla \times \mathbf{c}$. (A-35)

Written in tensor form, $\mathbf{c} \cdot \nabla \times \mathbf{c} = c_i e_{ijk} c_{k,j}$, where $c_i = e_{imn} b_m a_n$, since $\mathbf{c} = \mathbf{b} \times \mathbf{a}$

Thus

$$\begin{aligned} \mathbf{c} \cdot \nabla \times \mathbf{c} &= e_{imn} b_m a_n e_{ijk} c_{k,j} \\ &= e_{imn} e_{ijk} b_m a_n c_{k,j} \\ &= (\delta_{mj}\delta_{nk} - \delta_{mk}\delta_{nj}) b_m a_n c_{k,j} \\ &= b_j a_k c_{k,j} - b_k a_j c_{k,j}. \end{aligned}$$

We set $k = i$ since they are dummy variables to obtain

$$\mathbf{c} \cdot \nabla \times \mathbf{c} = a_i c_{i,j} b_j - b_i c_{i,j} a_j. \quad \text{(A-36)}$$

□

- $\mathbf{a} \cdot \nabla \times \mathbf{b}$. (A-37)

Written in tensor form, $\mathbf{a} \cdot \nabla \times \mathbf{b} = a_i e_{ijk} b_{k,j}$, where $a_i = e_{imn} c_m b_n$, since $\mathbf{a} = \mathbf{c} \times \mathbf{b}$.

Thus

$$\begin{aligned} \mathbf{a} \cdot \nabla \times \mathbf{b} &= e_{imn} c_m b_n e_{ijk} b_{k,j} \\ &= (\delta_{mj}\delta_{nk} - \delta_{mk}\delta_{nj}) c_m b_n b_{k,j} \\ &= c_j b_k b_{k,j} - c_k b_j b_{k,j} \\ &= -c_k b_j b_{k,j}. \end{aligned}$$

From the relationship $b_j c_{j,i} = -c_j b_{j,i}$ which was shown above, we arrive at

$$\mathbf{a} \cdot \nabla \times \mathbf{b} = b_j c_{k,j} b_k. \tag{A-38}$$

Also from (A-30),

$$\begin{aligned} \mathbf{a} \cdot \nabla \times \mathbf{b} &= b_k[c_{j,j} b_k + c_j b_{k,j} - c_k b_{j,j}] \\ &= b_k b_k c_{j,j} + b_k b_{k,j} c_{j,j} - b_k c_k b_{j,j} \\ &= c_{j,j}. \end{aligned}$$

Again j is a dummy variable hence we have

$$\mathbf{a} \cdot \nabla \times \mathbf{b} = c_{i,i}. \tag{A-39}$$

□

- $\mathbf{b} \cdot \nabla \times \mathbf{b}$. (A-40)

Written in tensor form, $\mathbf{b} \cdot \nabla \times \mathbf{b} = b_i e_{ijk} b_{k,j}$, where $b_i = e_{imn} a_m c_n$, since $\mathbf{b} = \mathbf{a} \times \mathbf{c}$.

Thus

$$\begin{aligned} \mathbf{b} \cdot \nabla \times \mathbf{b} &= e_{imn} a_m c_n e_{ijk} b_{k,j} \\ &= (\delta_{mj}\delta_{nk} - \delta_{mk}\delta_{nj}) a_m c_n b_{k,j} \\ &= a_j c_k b_{k,j} - a_k c_j b_{k,j}. \end{aligned}$$

Change the $k's$ to $i's$ since they are dummy variables

$$\mathbf{b} \cdot \nabla \times \mathbf{b} = c_i b_{i,j} a_j - a_i b_{i,j} c_j. \tag{A-41}$$

□

- $\mathbf{c} \cdot \nabla \times \mathbf{b}$. (A-42)

Written in tensor form, $\mathbf{c} \cdot \nabla \times \mathbf{b} = c_i e_{ijk} b_{k,j}$, where $c_i = e_{imn} b_m a_n$, since $\mathbf{c} = \mathbf{b} \times \mathbf{a}$.

Thus

$$\begin{aligned} \mathbf{c} \cdot \nabla \times \mathbf{b} &= e_{imn} b_m a_n e_{ijk} b_{k,j} \\ &= (\delta_{mj}\delta_{nk} - \delta_{mk}\delta_{nj}) b_m a_n b_{k,j} \\ &= b_j a_k b_{k,j} - b_k a_j b_{k,j} \\ &= b_j a_k b_{k,j}. \end{aligned}$$

Change the $k's$ to $i's$ since they are dummy variables

$$\mathbf{c} \cdot \nabla \times \mathbf{b} = a_i b_{i,j} b_j. \quad \text{(A-43)}$$

As shown in [16],

$$\mathbf{c} \cdot \nabla \times \mathbf{b} = c_i a_{i,j} c_j - a_{i,i}. \quad \text{(A-44)}$$

□

BIBLIOGRAPHY

[1] P.G. de Gennes, *The Physics of Liquid Crystals*, (Clarendon, Oxford, 1974).

[2] *Introduction to liquid crystals*, URL: http://plc.cwru.edu/tutorial/enhanced/files/lc/Intro.htm. [Accessed April 2007].

[3] I.W. Stewart, *The Static and Dynamic Continuum Theory of Liquid Crystals*, (Taylor and Francis, 2004).

[4] G.W. Gray and J.W. Goodby, *Smectic Liquid Crystals-Textures and Structures*, (Leonard Hill, 1984).

[5] M. Schadt and W. Helfrich, *Voltage-dependent optical activity of a twisted nematic liquid crystal*, Appl. Phys. Lett., **18**, 127-128, (1971).

[6] G.W. Gray and S.M. Kelly *Liquid crystals for twisted nematic display devices*, J. Mater. Chem., **9**, 2037 - 2050, (1999).

[7] *About Liquid Crystals*, URL: http://www.lci.kent.edu/lc.html. [Accessed April 2007].

[8] I.W. Stewart, *The alignment of smectic-A liquid crystals with director tilt on the boundaries.* J. Phys. A: Math. Theor. **40**, 5297-5318, (2007).

[9] I.W. Stewart, T Carlsson and F.M Leslie, *Chaotic instabilities in smectic-C liquid crystals*, Phys. Rev. E, **49**, 2130-2140, (1994).

[10] I.W. Stewart, E Momoniat, *Traveling waves in ferroelectric Smectic-C liquid crystals*, Phys. Rev. E, **69**, 061714, 1-9, (2004).

[11] M.A. Osipov and M.V. Gorkunov, *Ferroelectric ordering in chiral smectic-C* liquid crystals determined by nonchiral intermolecular interactions*, Phys. Rev. E. **77**, pp 031701, (2008).

[12] M.L.N. Madhu Mohan, B. Arunachalam and C.R. Aravindh Sankar, *Thermal and Electrical Characterization of a Ferro Electric Liquid Crystal*, (Springer Boston, 2008).

[13] M. Lines and A. Glass, *Principles and applications of ferroelectrics and related materials*, (Clarendon Press, Oxford, 1979).

[14] F.M. Leslie, I.W. Stewart and M. Nakagawa, *A continuum theory for Smectic-C liquid crystals* Mol. Cryst. Liq. Cryst., **198**, 443-454, (1991).

[15] X. Chean, *Notes on the Poisson-Boltzmann Equation*, (New York University, 2005).

[16] F.M. Leslie, I.W. Stewart, T. Carlsson and M. Nakagawa, *Equivalent smectic C liquid crystal energies*, Continuum Mech. Thermodyn. **3**, 237-250, (1991).

[17] I.W. Stewart, *Painlev analysis for a semi-linear parabolic equation arising in smectic liquid crystals*, IMA J. Appl. Math. 1998 **61**, 47-60, (1998).

[18] G.W. Bluman and S. Kumei, *Symmetries and Differential Equations*, (Springer-Verlag, New York, 1989).

[19] L.V. Ovsiannikov, *Group Analysis of Differential Equations*, (Academic, New York, 1982).

[20] G. W. Bluman and S. Kumei, *Symmetries and Differential Equations* (Springer-Verlag, New York, 1989).

[21] G. Baumann, *Symmetry Analysis of Differential Equations with Mathematica*, (Springer-Verlag, Berlin, 2000).

[22] A.D. Polyanin and V.F. Zaitsev, *Exact Solutions for Ordinary Differential Equations*, (CRC Press, Boca Raton, 1995).

[23] P. Grandclement, *Introduction to spectral methods*, (HAL-CCSd-CNRS, France, 2006).

[24] J.P. Boyd, *Chebysev and Fourier Spectral Methods*, (DOVER Publications Inc, New York, 2000).

[25] H. Takenaka, Y. Wang and T. Furumura, *An efficient approach of the pseudospectral method for modelling of geometrically symmetric seismic wavefield*, Earth Planets Space, **51**, 73-79, (1999).

[26] B Fornberg, *The pseudospectral method: Accurate representation of interfaces in elastic wave calculations*, Geophysics, **53**, 625-637, (1988).

[27] R. Renaut and J. F. Hlich, *A Pseudospectral Chebychev Method for the 2D Wave Equation with Domain Stretching and Absorbing Boundary Conditions*, Journal of Computational Physics, **124**, 324-336, (1996).

[28] J. Lund and K. L. Bowers, *Sinc Methods for Quadrature and Differential Equations*, SIAM, (1992).

[29] N Bellomo, *Nonlinear Models and Problems in Applied Sciences from Differential Quadrature to Generalized Collocation Methods*, (Torino, Italy, 1997).

[30] F. Stenger, *Numerical Methods based on Whitaker Cardinal, or Sinc Functions*, SIAM Review **23**(2), 165-224, (1981).

[31] J.A.C. Weideman and S. C. Reddy, *A MATLAB Differentiation Matrix Suite*, ACM Trans. Math. Software, **26**(4), 465-519, (2000).

[32] H. Holmas, D. Clamond and H. P. Langtangen, *A Pseudospectral Fourier Method for a 1D Incompressible Two-Fluid Model*, International Journal for Numerical Methods in Fluids, (2007).

[33] I.M.B. Nielsen and C.L. Janssen, *A novel pseudospectral Fourier method for solving Poisson's equation for a solute in a non-uniform dielectric*, Computer Physics Communications, **136**(1), 29-36, (2001).

[34] J.P. Boyd, *Chebyshev and Fourier Spectral Methods, Second Edition*, (Michigan, 2000).

[35] M.N.O Sadiku and C.N. Obiozor, *A simple introduction to the method of lines,* Int. J. Elec. Eng. Educ., **37**(3), 282-296, (2000).

[36] D. R. Durran, *Numerical Methods for Wave Equations in Geophysical Fluid Dynamics*, (Springer-Verlag, 1999).

[37] S. Ried, H. Pleiner and W. Zimmermann, *Electrically driven hybrid instabilities in smectic C liquid crystal films*, Europhys. Lett., **52**(5),

525-531, (2000).